## ABSTRACT

Title of Thesis: **Synthesis and Characterization of Hemostatic Foams**

**Michael Brendan Rudy, Master of Science, 2018**

Directed by: Prof. Srinivasa R. Raghavan
Department of Chemical & Biomolecular Engineering

Hydrophobically modified (hm) derivatives of biopolymers like chitosan have the ability to coagulate blood cells and thus stop bleeding from severe injuries (i.e., achieve hemostasis). Our lab has been particularly interested in developing foams based on these polymers for use as hemostastic agents. Foams are attractive because an expanding foam at a wound site can counteract blood loss without the need for mechanical compression. The amphiphilic nature of hm-polymers also enables them to stabilize such foams. Previous work centered around a foam based on hm-chitosan (hmC) that was delivered out of a canister. To effectively combat internal hemorrhaging, we recognized the need to develop foams that could be more precisely placed at the wound site and also had greater mechanical integrity. Towards this end, this thesis describes a new class of polymeric foams that can be delivered out of a double-barreled syringe (DBS) by combining precursors in the two barrels that produce bubbles of $CO_2$ gas *in situ*. Moreover, we show that by combining hmC in one barrel with a second biopolymer – hm-alginate (hmA) – in the other, we can generate foams with enhanced rheological properties compared to foams of hmC alone. This rheological enhancement is quantified in our work, and is due to electrostatic interactions between the cationic hmC and the anionic hmA chains. Preliminary studies in animal wound models also confirm that hmC-hmA foams can be precisely directed to a wound using the DBS and that these foams form effective barriers to blood loss due to their greater mechanical integrity.

# SYNTHESIS AND CHARACTERIZATION OF HEMOSTATIC FOAMS

**By**

Michael Brendan Rudy

Thesis submitted to the Faculty of the Graduate School of the
University of Maryland, College Park, in partial fulfillment
of the requirements for the degree of
Master of Science
2018

**Advisory Committee:**

Prof. Srinivasa R. Raghavan, Dept. of Chemical & Biomolecular Engineering, Chair

Prof. Amy J. Karlsson, Dept. of Chemical & Biomolecular Engineering

Prof. Taylor J. Woehl, Dept. of Chemical & Biomolecular Engineering

**Dedication**

I dedicate this thesis to my Mother and Father.

**Acknowledgements**

Firstly, I would like to acknowledge and thank Dr. Raghavan for his guidance and support throughout the entirety of my masters research.

Secondly, I want to acknowledge Dr. Matthew Dowling for his support, guidance and mentoring through the research process.

I also would like to acknowledge the other members of the complex fluids and nanomaterials group such as Trip, Brady, Ankit, Kerry, Niti, So Hyun, James, Tonya, Leah, Brandon, Xiu, Hema, Ben and Nikhil. Everyone was very supportive and help provide guidance though my process

Lastly, I want to acknowledge the undergraduate students who helped me over the years: Ryan, Joey, Michael and Claire. You all were a joy to work with and were tremendous help.

## Table of Contents

## List of Figures

## **Chapter 1:** INTRODUCTION & OVERVIEW

Severe trauma is a leading cause of death for soldiers on the battle field and for civilian young adults.[1-4] Uncontrolled hemorrhaging, or severe blood loss, is responsible for the majority of trauma related deaths.[5] For example, 40% of deaths within the first 24 h of injury are due to hemorrhaging,[6] and between 33 to 56% of these deaths occur before the injured person can make it to a hospital.[7] Hemorrhages are typically classified into two kinds. Compressible hemorrhages are bleeding injuries to the body extremities, and these are treatable by an external hemostatic agent (i.e., a material to stop bleeding) that is applied using direct compression. Non-compressible (intracavity) hemorrhages are injuries to areas where compression cannot be directly applied. Medical advancements in external hemostats have led to much higher survival rates for compressible hemorrhages; however treatment for non-compressible hemorrhaging has lagged behind. For example, one study found that non-compressible hemorrhages account for 85% of fatalities in otherwise survivable injuries on the battlefield.[2]

A promising approach to combat non-compressible hemorrhaging is by the use of a sprayable foam. Holcomb *et al*. originally hypothesized that the expansion of foams (with an active hemostatic agent) in the wound cavity would allow for bleeding to be arrested without direct pressure.[8] Initial hemostatic foams were based on the blood-clotting protein, fibrin, but these have not proved practical due to the high cost of recombinant human proteins and cumbersome requirements for the storage and preparation of the corresponding foams.[9,10] As an alternative, our lab has developed sprayable foams based on derivatives of the widely available biopolymer, chitosan.[5,6]

This work is described below, and as a prelude, we will first describe our contribution to the field of hemostatic materials.

The starting point for our work on hemostatic materials was our discovery that a chitosan derivative, *viz*. hydrophobically modified chitosan (hmC), was able to convert liquid blood into a self-supporting gel.[11-20] This gelling ability arose because hmC chains inserted their hydrophobic tails into the membranes of blood cells (via hydrophobic interactions) and thereby connected the blood cells into a three-dimensional network.[11,12,19,21] This blood-gelling ability is similar to the clotting of blood by networks of fibrin. Subsequently, hmC-based bandages were shown to arrest bleeding from severe hemorrhage in pig injury models.[22] The blood-gelling ability was related to the presence of hydrophobic groups along a polymer backbone. Thus, other polymers with hydrophobes, such as hydrophobically modified alginate (hmA) could also gel blood; additionally, hmA could also stop bleeding in animal models.[23] A key difference between the parent polymers, chitosan and alginate, is that chitosan is cationic while alginate is anionic.[24]

With regard to hemostatic foams, our lab's previous work exploited the amphiphilic nature of hmC to create a surfactant-free foam (see Section 2.5 in Chapter 2).[5] The foam was delivered through a canister containing a propellant (to generate gas bubbles) and an hmC solution. When the foam was sprayed from the canister nozzle, gas bubbles became stabilized by hmC chains. The foams were tested on a bleeding pig liver model, and were shown to be able to achieve sustained hemostasis for an hour without

compression.[5] Note that the hmC had a dual purpose in the foam, serving as both the hemostatic agent that interacted with blood cells as well as the stabilizer of bubbles in the foam.

Our previous work with hemostatic foams is encouraging, but we have recognized the need for certain improvements in foam properties. While the canister-based hmC foam is ideal for external spray application, it produces a foam that spreads over an appreciable area (much like a shaving foam). This provides less control for combating internal hemorrhages; when the foam has to be applied to an internal wound through an open cavity, it is often necessary to direct it to a precise location. Moreover, the foam should ideally persist at that location for sufficient time to allow the active ingredient (e.g., hmC) to interact with blood and arrest its flow. The hmC foam, however, tends to be mechanically (i.e., rheologically) weak, and can get pushed aside by flowing blood. Thus, a foam with a different consistency – one that is more robust and forms a better mechanical barrier – is needed.

In this thesis, we describe a new type of hemostatic foam that addresses both the above issues. First, to direct the foam to a precise point, we use a double-barreled syringe (DBS) to generate a foam *in situ*. One barrel of the syringe contains an acidic solution (acetic acid) while the other barrel contains a basic solution (sodium bicarbonate). The acid and base mix together at the tip of the DBS and their reaction generates carbon dioxide ($CO_2$) gas in the form of bubbles. The bubbles are stabilized by polymers present in one or both the solutions. The result is a foam whose volume and extent can be

regulated by the size of the DBS nozzle. Also, the placement of the foam can be precisely controlled by positioning the DBS at the right location.

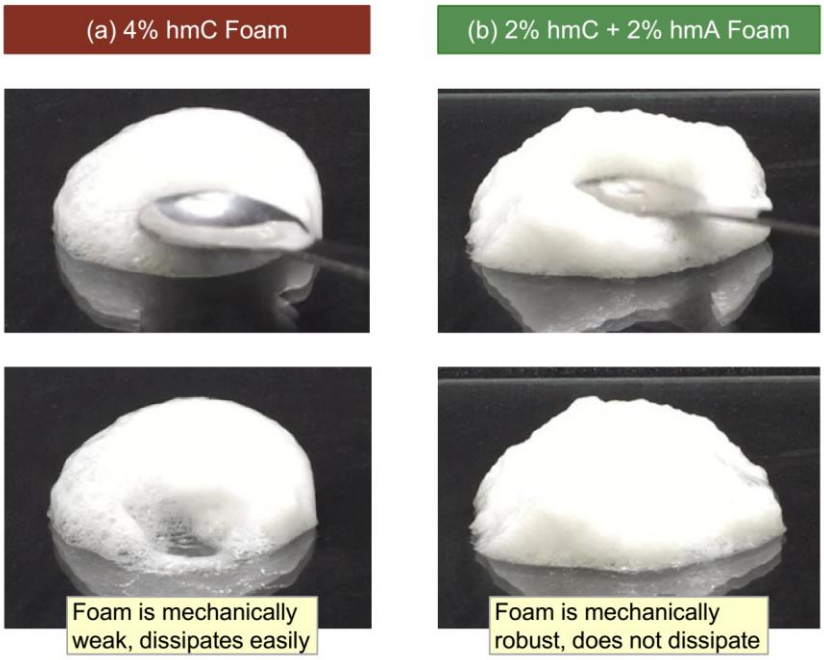


**Figure 1.1**: **Comparison of foams prepared in this study.** In (a), a foam made using hydrophobically modified chitosan (hmC) alone is shown. In (b), a foam based on hmC combined with hydrophobically modified alginate (hmA) is shown. The latter is more robust and resists deformation. The photos show that when the foam in (a) is tapped with a spatula, it gets deformed and dissipates over that area. When the foam in (b) is similarly manipulated with a spatula, it does not dissipate; rather it responds like an elastic object.

Next, we show that the mechanical robustness of the foam can be enhanced by the *combined use* of two hemostatic biopolymers, hmC and hmA, in the two barrels of the DBS. The hmC is dissolved in the acetic acid and the hmA in the sodium bicarbonate. When the solutions mix, the hmC and hmA come into contact and form a gel-like material via electrostatic interactions between the oppositely charged polymers.[24] The result is a "gel-foam" that is more robust than a foam of hmC alone (Figure 1.1). The differences in rheological properties between hmC foams vs. hmC-hmA foams became

evident qualitatively through a series of benchtop studies. We then set out to systematically characterize these differences using rheological techniques. Thereafter, we also study the microstructures in these foams using optical microscopy. Finally, we have conducted preliminary experiments on the use of these foams in animal wound models. We confirm that hmC-hmA foams can be precisely directed to a wound using the DBS and that these foams form effective barriers to blood loss due to their greater mechanical integrity.

## 2.1 Chitosan and Hydrophobically-Modified Chitosan

Chitin, a polysaccharide present in the cell walls of fungi and the shells of crustaceans, is the precursor to chitosan. Its repeat units are N-acetylglucosamine groups. Alkaline hydrolysis of chitin deacetylates the backbone and forms chitosan. The deacetylation usually does not remove all acetyl groups, with the remaining fraction termed the degree of acetylation (DA). As shown in Figure 2.1a, this gives chitosan a random distribution of β-(1→4)-linked D-glucosamine (deacetylated) units and N-acetyl-D-glucosamine (acetylated) units. Below a pH of 6.5, chitosan is soluble in aqueous solutions, as the amines alone the backbone get protonated, which makes the polymer cationic.[25-27] Chitosan has antimicrobial properties due to its cationic nature.[25,26,28]

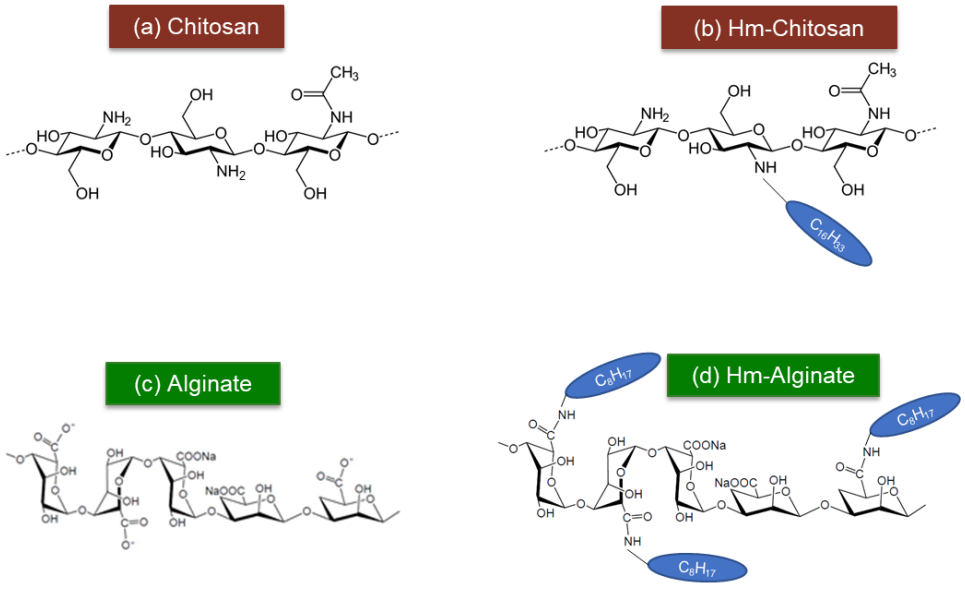


**Figure 2.1**: **Chemical structures of polymers involved in this study:** (a) chitosan, (b) hydrophobically modified chitosan (hmC) with $C_{16}$ hydrophobic side chains, (c) alginate and (d) hydrophobically modified alginate (hmA) with $C_8$ hydrophobic side chains.

Hydrophobically modified chitosan (hmC) is synthesized via the reaction of an R-anhydride with some of the amines on the chitosan backbone.[19,21] The reaction changes the amine group ($NH_2$) to an NH-R group. The R group is usually an alkyl tail (with lengths from $C_1$ to $C_{18}$); see Figure 2.1b. The degree of hydrophobic modification (i.e., the fraction of amines with an R group) can be controlled by the stoichiometry of the reacting mixture. Due to associations between the hydrophobes, hmC chains form a transient network, and this renders the aqueous solutions viscous. The longer the hydrophobic tail and the higher the degree of hydrophobic modification the higher the viscosity of the hmC solution. However, if these two parameters are too high, the hmC will be insoluble, even at low concentrations. The hmC variants in our studies typically have $C_{12}$ to $C_{16}$ tails and the degree of modification is 1 to 6%.[22]

## 2.2 Alginate and Hydrophobically-Modified Alginate

Alginate is a linear polysaccharide that is a large component of the cell walls of brown algae. It is composed of (1-4)-linked β-D-mannuronate (M) and α-L-guluronate (G) residues (Figure 2.1c).[24] These residues can be in random sequences or in blocks of consecutive M or G sequences, with the composition being dependent on the algal species. Alginate is known to be biologically compatible and is widely used in the food, medical and textile industries. It is often used as a thickening agent because it forms physical gels when combined with divalent cations like $Ca^{2+}$.[23] Alginate has been used in FDA-approved biomedical products. Hydrophobically modified alginate (hmA) can be produced by reacting alginate with alkyl amines using a coupling agent.[28] For example, if the amine is octylamine, $C_8$ hydrophobes are added to alginate backbone (Figure 2.1d).

The degree of hydrophobe modification is typically ~ 25%, which is higher than in the case of hmC.[23]

### 2.3 Studies on hmC and hmA Combined with Vesicles, Blood, and Other Cells

Previous work in our lab has studied both hmC and hmA in combination with suspensions of vesicles, blood cells, and other mammalian cells.[21,29] Note that vesicles are nanoscale spheres formed by self-assembly of amphiphilic molecules (lipids or surfactants); they have a bilayer of the amphiphiles enclosing an aqueous core. The cells also have bilayer membranes enclosing their internal contents. In all cases, the samples were thin, flowing liquids prior to addition of the polymers. However, upon addition of hmC or hmA, the samples were converted to physical gels that exhibited elastic rheology and held their weight in inverted tubes or vials (Figure 2.2). Scattering and microscopy techniques confirmed that the structures in the original sample remained intact upon adding the polymers. This suggested a mechanism for gelation based on polymer bridging, as shown in Figure 2.2. That is, the hydrophobes on the polymer chains are believed to insert themselves into the bilayers enclosing the vesicles or cells (note that the bilayers have a hydrophobic core of lipids between the hydrophilic headgroups on either side).[21] When chains insert hydrophobes into the bilayers of adjacent structures, they end up bridging the structures into a 3-D network (Figure 2.2). Gelation is thus due to weak, physical bonds (hydrophobic interactions).

Support for the above mechanism comes from a series of studies. First, the parent polymers (chitosan, alginate) do not induce a gel, implying that the hydrophobes are

necessary for gelation.[23] Second, gelation can be reversed by adding a supramolecule called α-cyclodextrin (α-CD), which has a hydrophobic pocket.[19,29] When introduced to a sample gelled by hmC or hmA, α-CD ungels the mixture and reverts it to a thin liquid. This occurs because the binding pocket in α-CD sequesters the hydrophobic tails on the polymer chains, thereby undoing the 3-D network. The ungelling by α-CD further proves that free hydrophobes are required for gelation.

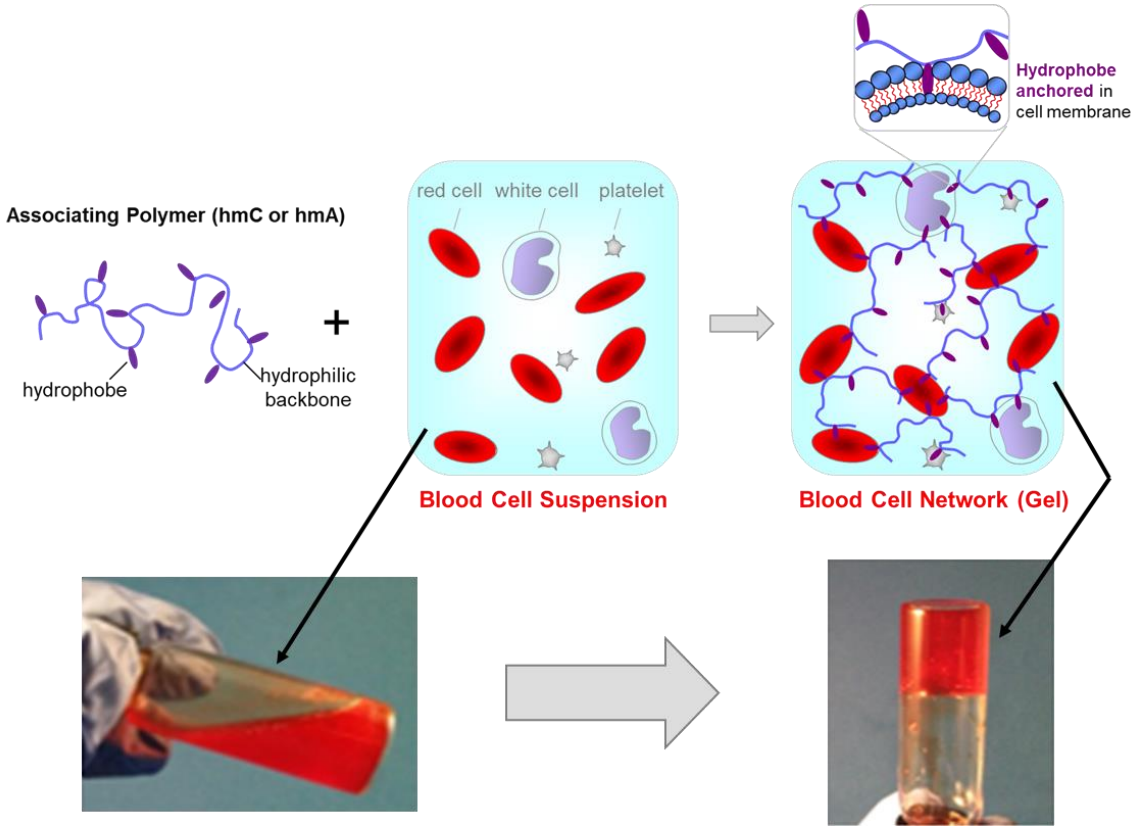


**Figure 2.2**: **Blood gelation by hydrophobically modified polymers like hmC and hmA.** Initially, the blood is a flowing liquid with the cells being discrete structures (photo on the left). When the polymer is added, the sample is converted into a gel that holds its weight in the inverted vial (photo on the right). The schematic shows the hypothesized structure of the gel, which is a network of cells bridged by polymer chains. The driving force for polymer-cell interaction is the interaction between the hydrophobic tails on the polymer with the hydrophobic interior of cell bilayers. Adapted from Refs. 19 and 29.

## 2.4 Foams: Properties and Classification

Foams are formed by trapping bubbles of gas in a liquid or solid; the corresponding materials are termed liquid and solid foams, respectively.[30-35] Our work is focused on liquid foams. The bubbles are typically stabilized by surfactant molecules, whose hydrophilic heads are oriented in the liquid phase, while the hydrophobic tails extend into the gas phase.[30] A liquid foam displays characteristics of all three states of matter, behaving like a solid at small extents of shear, flowing like a liquid at larger extents of shear, and changing its volume like a gas in response to temperature and pressure changes. The mechanical (rheological) properties of liquid foams are characterized by bulk and shear moduli.[30-35] The bulk modulus is mostly dictated by the gas phase in the foam. The shear modulus, on the other hand, is dictated by the bubble size, which itself is affected by the liquid's surface tension and viscosity.[34,36] Smaller bubble sizes correspond to longer drainage times, leading to longer foam stability.

In terms of their rheology and structure, liquid foams can be classified as billowing, lacy, and capious foams. A billowing foam is one with large, polydisperse bubbles and a relatively low bubble volume fraction (in turn, the liquid fraction is relatively high). On the other extreme, a capious foam has small, tightly-packed bubbles, with the bubble volume fraction being very high. Such a foam displays the characteristics of a solid and is able to resist higher levels of shear. A lacy foam lacks the tightness and density of capious foam but has less liquid characteristics than a billowing foam. This leads to lacy foams being referred to as "dry foams", as the liquid membranes between bubbles are very thin and the foam lacks mechanical strength.[37] Over time, capious foams

often become lacy or billowing foams as the gas escapes or the bubbles coalesce. The timeframe of this transformation affects the stability of the foam.

### 2.5 Previous Research on hmC-Based Hemostatic Foams

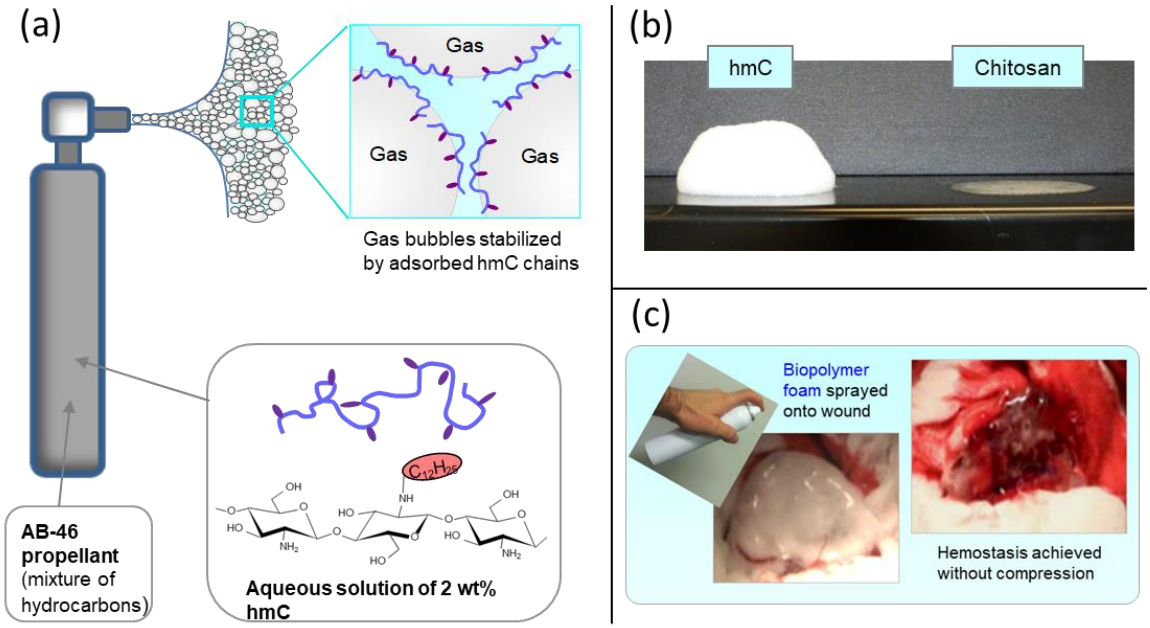


**Figure 2.3: Formulation of a foam based on hmC, and its function as a hemostatic agent.** (a) Schematic of the canister used to deliver the foam. The canister contains a propellant and an aqueous solution of hmC. A liquid foam is ejected from the canister; in this foam, gas bubbles are stabilized by hmC chains. The chains adsorb on the bubbles with their hydrophobes oriented towards the gas phase. In the absence of hydrophobes, the parent polymer (chitosan) does not create a stable foam, as shown by the photo in (b). (c) The foam is sprayed onto a bleeding liver injury in a pig model, whereupon it stops the bleeding without the need for compression. Adapted from Ref. 5.

As noted in the Introduction, foams are attractive as hemostatic agents for use against non-compressible injuries. Our lab has previously created foams based on hmC and tested their hemostatic efficacy. The foam was delivered through a canister containing a propellant and an hmC solution (Figure 2.3a). When the foam was sprayed from the canister nozzle, bubbles of propellant gas were formed, which became stabilized

by hmC chains, as shown in Figure 2.3a. That is, the hmC chains, being amphiphilic, function just like surfactant molecules: the chains adsorb at the interface of the gas bubbles in such a way that their hydrophobic tails all extend into the gas phase, while the hydrophilic backbone orients towards the aqueous phase. The result is a foam that has sufficient stability even in the absence of additional surfactant. In the absence of hydrophobes, the parent polymer (chitosan) cannot stabilize gas bubbles, which then dissipate away into a thin liquid within seconds (Figure 2.3b). The above hmC foam was tested against a bleeding liver injury in pigs. When sprayed onto the wound, the foams achieved hemostasis for the duration of the experiment (1 h) without any external compression.[5,6] The ability to achieve hemostasis is related to the blood-gelling ability of the active ingredient (hmC), as well as the ability of the foam to expand and fill the wound site and also form a temporary mechanical barrier that counteracts blood loss.[8] All in all, our previous work shows that hmC foams can be quite effective for treating non-compressive hemorrhaging. Note that the hmC has a dual purpose in these foams, serving as both the hemostatic agent as well as the foam stabilizer.

### 2.6 Interactions Between Chitosan and Alginate

As noted above, chitosan is a cationic polymer due to its amines, while alginate is an anionic polymer due to its carboxylates.[23] When chitosan and alginate come into contact they form a polyelectrolyte complex (PEC) through electrostatic interactions.[24] If solutions of the two polymers are mixed vigorously, the PEC will exist as suspended particles in the mixture, and with time, these particles will settle to form a precipitate (Figure 2.4b). However, if a solution of chitosan is added dropwise into a solution of

alginate (or vice versa), then the PEC will form at the droplet interface. The droplet will thereby be covered by a PEC membrane, i.e., it will become a capsule (Figure 2.4a). Indeed, such a scheme to generate capsules using chitosan and alginate (as well as other pairs of oppositely charged polymers) has been used extensively in our lab. The same interactions also occur between hmC and hmA; in fact, the hydrophobic interactions add on and strengthen the electrostatic interactions. Thus, if solutions of hmA and hmC are mixed vigorously, they will immediately form a gel-like PEC (Figure 2.4c).

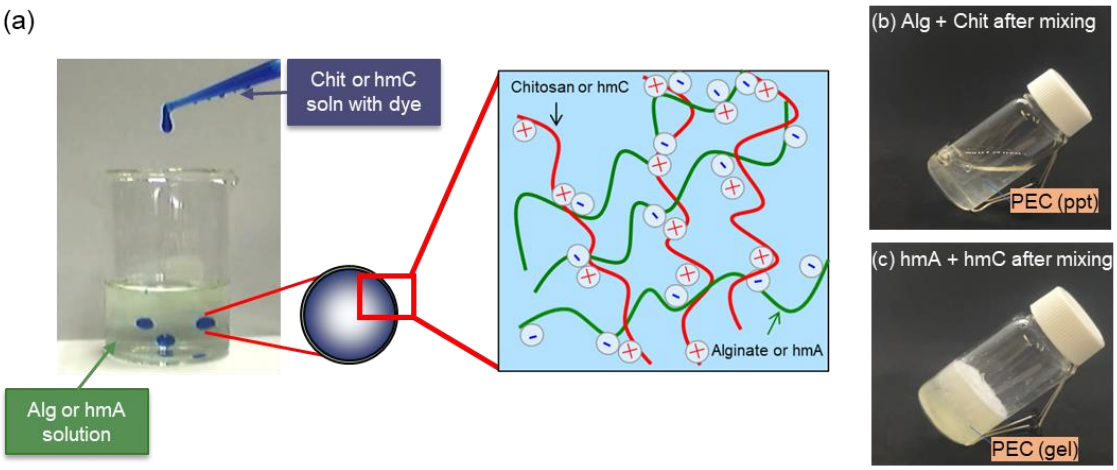


**Figure 2.4: Evidence of electrostatic interactions between chitosan and alginate (as well as their derivatives)**. (a) When drops of chitosan (Chit) are introduced into a solution of alginate (Alg), the polymers bind to each other via electrostatic interactions, forming a polyelectrolyte complex (PEC), as shown in the inset. This results in the droplets being converted into capsules. (b) When solutions of Alg and Chit are mixed together, the PEC exists as suspended particles or precipitates. (c) When solutions of hmA and hmC are mixed together, the PEC is even stronger, and the entire sample is converted into a solid-like gel.

## 2.7 Rheology

Rheology is the study of the deformation and flow of matter. Rheological measurements are performed under steady shear or dynamic oscillatory shear. Steady

shear rheology subjects the sample to a constant shear rate $\dot{\gamma}$ and the materials response is measured as a shear-stress $\sigma$. This allows for the apparent viscosity $\eta$ to be calculated as the ratio of $\sigma / \dot{\gamma}$. By varying the shear-rate, a flow curve, i.e. a plot of viscosity vs. shear-rate is obtained for the sample.

Dynamic rheology characterizes the response of the material to a sinusoidal strain $\gamma = \gamma_0 \sin(\omega t)$, with $\gamma_0$ being the amplitude and $\omega$ the frequency of the oscillations. The response is a sinusoidal stress, $\sigma = \sigma_0 \sin(\omega t + \delta)$ that can be decomposed into terms that are in- and out-of-phase with the strain: $\sigma = G'\gamma_0 \sin(\omega t) + G''\gamma_0 \cos(\omega t)$. The elastic modulus $G'$, also called the storage modulus, gives insight into the elastic or solid-like nature of the material, i.e., how it stores the strain energy. The viscous modulus $G''$, also called the loss modulus, gives insight into the viscous or liquid-like nature of the material, i.e., how it dissipates the strain energy. Dynamic tests must be run in the "*linear viscoelastic*" (LVE) regime of the sample, which is the range over which the stress is linearly proportional to the strain. As long as the imposed strain is within the LVE region, the moduli will be functions only of the frequency $\omega$ and will be true material functions. A plot of $G'$ and $G''$ vs. $\omega$ is called the frequency spectrum of the material, and it is a signature of the structure present in the material. Typically, foams show elastic behavior, i.e., their $G' > G''$ over the entire range of $\omega$, with both moduli being independent of $\omega$. When studying foams, tests are usually done using a parallel-plate geometry, with the plates being covered by sandpaper to minimize wall slip.

# **Chapter 3:** HEMOSTATIC FOAMS BASED ON MIXTURES OF HYDROPHOBICALLY MODIFIED BIOPOLYMERS

## 3.1 Introduction

Our lab has previously developed hemostatic foams based on hydrophobically modified chitosan (hmC) and shown these to be effective at treating hemorrhaging injuries without compression.[5,6] These foams were delivered out of a canister filled with a propellant (see Section 2.5). When the sample ejected from the nozzle of the canister, the propellant volatilized and form bubbles, which became stabilized by hmC chains, leading to a foam. The foam was delivered to a bleeding wound by pointing the nozzle and pressing the trigger. As the ejected foam made contact with a receiving surface, it covered a relatively wide area, typically at least around 1 $cm^2$. Due to foam expansion, this area tended to increase with time as well. In experiments with bleeding animal models, our lab found that foams delivered out of a canister could rapidly cover a large bleeding injury. At the same time, the foam film covering the wound was also relatively weak and would sometimes be breached by flowing blood out of the wound.

Our experiments indicated that there are two areas of improvement needed with our foams. First, there is a need to direct the foams with greater precision than is possible with the canister. This is particularly important in the case of internal bleeds, such as due to a cut or tear in a blood vessel or an internal organ. In these cases, the canister foam tends to spread over too wide an area whereas it would be better served if the foam were localized to the injured area. Second, with regard to staunching the blood flow out of the wound, there is a need for the foam to remain in place for sufficient time. For this, the

mechanical properties of the foam are also important, i.e., the foam must initially serve as a mechanical barrier to blood flow. This would allow the active hemostatic ingredient (hmC) to interact with blood cells, and also for the components of the body's clotting cascade to collect and concentrate underneath the foam film. In short, there is a need for a foam with greater mechanical integrity compared to the previous hmC foams.

To achieve the above objectives, we first describe a new mode for foam delivery using a double-barrel syringe (DBS). The DBS provides greater precision in foam placement compared to the canisters used earlier. Second, with regard to creating more robust foams, we hypothesized that this could be achieved by the *combined use* of two hemostatic biopolymers, hmC and hydrophobically modified alginate (hmA), in the two barrels of the DBS. Both hmC and hmA have been shown to gel blood due to the insertion of their hydrophobes into blood-cell membranes, which leads to a 3-D network of the cells (Section 2.3).[19,23] Also, as noted in Section 2.6, hmC and hmA are respectively cationic and anionic, and the strong electrostatic interactions between them gives rise to a polyelectrolyte complex (PEC).[24] We hypothesized that PEC formation would enhance the rheology of the foam, and this is confirmed by rheological measurements. We have also characterized the structure of hmC-hmA foams relative to those of hmC alone using optical microscopy. Finally, we have conducted preliminary studies on the use of these foams in bleeding animal models. We confirm that hmC-hmA foams can be precisely directed to a wound using the DBS and that these foams form effective barriers to blood loss due to their greater mechanical integrity.

### 3.2 Experimental

**Materials**. Chitosan (Medium Molecular Weight, 250-400 kDa, 99% deacetylated, Product Code 43020) was obtained from Primex Corp. (Iceland). Sodium alginate (product number A2033, sourced from brown algae, molecular weight of 80–120 kDa), N-(3-dimethylamino-propyl)-N-ethylcarbodiimide hydrochloride (EDC), n-octylamine (99%), Hydrochloric Acid (HCl) and Sodium Hydroxide (NaOH) were obtained from Sigma Aldrich. Palmitic ($C_{16}$) anhydride (96.0%) and Acetic Acid ($CH_3COOH$) were obtained from TCI America. Arm & Hammer Pure Baking Soda was the source of Sodium Bicarbonate ($NaHCO_3$), note pure baking soda is 100% $NaHCO_3$. Bovine heparinized blood was sourced from Lampire Biological Products. Commercial foams used were Caress Botanicals Shower Foam and Gillette Foamy Shaving Foam.

**Synthesis of hmC and hmA.** To synthesize hmC, 1 wt% chitosan was first dissolved in 0.2 M acetic acid.[19] An equal volume of ethanol was then added and the solution was heated to 65°C. Palmitic anhydride was dissolved in a separate beaker with ethanol and heated to 65°C. The anhydride solution was then added to the chitosan solution such that the stoichiometry corresponded to 1.5 mol% of the amines on the chitosan. The mixture was allowed to react overnight, whereupon the hmC was formed. To precipitate the hmC from this solution, the pH was raised by adding NaOH. The precipitate was then washed with ethanol several times and left to dry, then ground into a powder. The resulting hmC had $C_{16}$ hydrophobes with a degree of hydrophobe modification of 1.5%.

To synthesize hmA, 2 wt% alginate was dissolved in water using HCl to make the solution acidic (with a pH of approximately 3.4).[23] An aqueous solution of EDC (0.66 grams of EDC for every gram of alginate) was then added to this solution, followed by the addition of n-octylamine (0.91 grams of octylamine for every gram of alginate) dissolved in 50/50 water/ethanol. The reaction was allowed to run for 24 h to form the hmA. The hmA was precipitated out by adding acetone into the reaction mixture. This precipitate was then washed several times with acetone and allowed to dry, then ground into a powder. The resulting hmA had $C_8$ hydrophobes with a degree of hydrohobe modification of 25%.

**Double-Barreled Syringe Preparation.** The double-barreled syringes were obtained from J Dedoes, Inc. The dimension of the barrel and plunger of the syringe were 3mL x 3 mL. The mixing tip of the syringe was a 3 mm x 16 Element – Blunt Tip. Different solutions were loaded into the two barrels (2 mL of solution into each barrel). In one barrel, a solution of hmC dissolved in 1.1 M $CH_3COOH$ at specific concentrations was used. In the other barrel, the solution was either 1.1 M $NaHCO_3$ or hmA dissolved in it at specific concentrations.

**Optical Microscopy.** A small amount of a given foam was injected onto a glass slide and allowed to sit for a few minutes. Images were then captured on an Olympus IX51 microscope at 100× and 400× magnification using a Hamamatsu A3472-06 camera. Bubble size distributions were analyzed using the ImageJ program. For each formulation at least three 1.13×0.86 mm images were analyzed.

**Blood experiments.** The syringe was loaded with 2 mL of acidic solution and 2 mL of basic solution (4 mL total). Blood was added to a 50 mL centrifuge tube then foam was injected into the tube so that it hit the surface of the blood. After the foam had expanded the tube was inverted and held upside down until the majority of the blood flowed through. The time it took for the blood to flow through was recorded. Initial tests used 10 mL of blood. When foam formulations successfully held back blood for extended periods of time the amount of blood was increased, up to 20 mL.

**Rheology Frequency and Stress Sweeps.** All rheological tests were performed on a TA Instruments AR2000 stress-controlled rheometer. All experiments were done at 25 °C using parallel plate geometry (plate diameter was 40 mm). The top and bottom surfaces had 24-grit sandpaper fixed to them. Dynamic frequency and stress spectra were tested in the linear viscoelastic regime of the sample. The linear viscoelastic regime was evaluated by prior dynamic strain sweeps. Both frequency and stress sweeps were completed in under five minutes.

**Compression Tests.** A TA Instruments AR2000 stress-controlled rheometer was used for compression testing. The same temperature and plate setup used for frequency and stress sweeps were used for compression testing. The squeeze/pulloff test mode was selected in the rheometer software. A 3D printed cylinder, with an interior diameter of 40.2 mm, was placed on the bottom plate. The cylinder was positioned so that the top plate could pass through the cylinder without touching the walls. This was done to keep the foam between

the two plates, because without the cylinder the foam would simply push out from between the plates as it was compressed. The foam was loaded into the cylinder then the top plate was brought down to a predetermined height. This was done to account for variations in foam expansion between tested foams. Once the test was started the top plate came down at a constant rate so that the test time was less than five minutes.

**Animal Studies.** All animal studies were outsourced to gel-e and performed by the company at Noble Life Sciences under gel-e's approved IUCAC protocol. An immature female Yorkshire swine (38 kg) was used in this study. The animal was housed in a climate controlled facility consistent with protocols approved by the Association for Assessment and Accreditation of Laboratory Use Committee of Noble Life Sciences (Sykesville, MD). Food and water were available *ad libitum*. All animals received care in strict compliance with the National Research Council's Guide for Care and Use of All Laboratory Animals.

A liver injury, modeled after a standard parenchymal injury, was created by making multiple 10 mm (diameter) × 5 mm lesions using a punch biopsy (Acu-Punch Biopsy Punch (sterile), 10 mm, Fisher Scientific). Biopsies were created in both the liver and spleen on available surface, while the animal remained within 5% of the baseline mean arterial pressure (63 mm Hg). The biopsy punch injury denotes the start of the prehospital phase (time 0). After 30 sec of free bleeding, the foam was applied to the biopsy site; 2 mL of foam was applied to each biopsy site. The injury site was then observed for hemostasis: the achievement of hemostasis was defined as lack of visible bleeding

through or around the edges of the foam after 2 min. The total observation time per experiment was 60 min. In cases where hemostasis was not achieved within the 2 minute window, the bleed was stopped by cauterization. In this way, it was possible to make multiple injuries on one liver and spleen while still retaining the blood pressure of the pig to keep bleed rates consistent.

### 3.3 Results and Discussion

Schematics of the double-barreled syringe (DBS) are shown in Figure 3.1. The DBS generates foam *in situ* via the reaction of an acidic solution (acetic acid, $CH_3COOH$) and a basic solution (sodium bicarbonate, $NaHCO_3$) loaded in separate barrels. The two solutions come into contact at the mixing tip, whereupon the following reaction occurs:

$$CH_3COOH + NaHCO_3 \rightarrow CH_3COONa + CO_2\,(g) + H_2O \qquad (1)$$

Thus, the net outcome is the formation of carbon dioxide ($CO_2$) gas in the form of bubbles. As long as there is a surfactant or an amphiphilic polymer in at least one of the barrels, the bubbles are likely to get stabilized and thereby a stable foam can be produced out of the DBS.

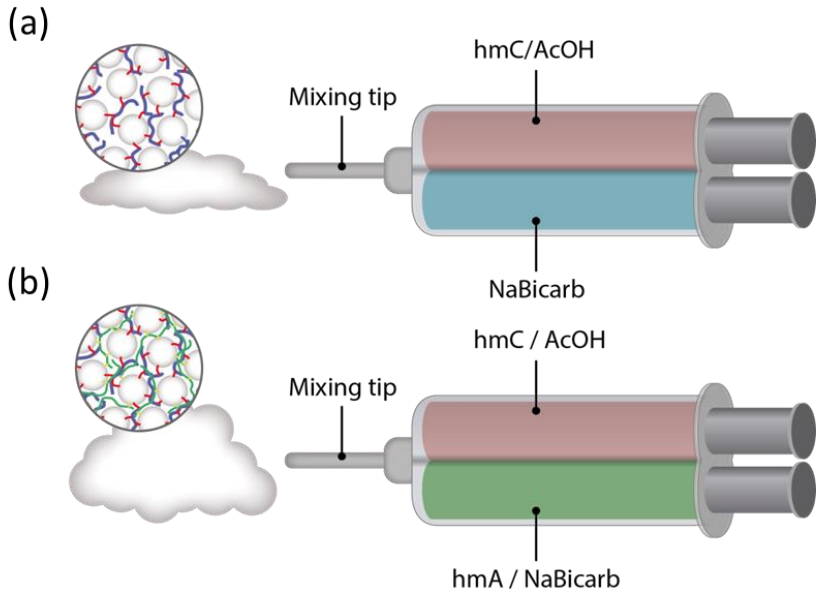


**Figure 3.1: Delivery of hemostatic foams using a double-barreled syringe (DBS).** Two kinds of foams are compared. In (a), one barrel has a solution of hmC in acetic acid ($CH_3COOH$), while the other has a solution of sodium bicarbonate ($NaHCO_3$). In (b), the first barrel is the same as in (a) while the other barrel has a solution of hmA in $NaHCO_3$. In both cases, at the mixing tip, a foam of $CO_2$ is generated by Reaction (1). The insets show that the bubbles in the foam are stabilized by the amphiphilic hmC in (a) and by hmC and hmA in (b).

Figure 3.1 also contrasts the two main kinds of foams created using the DBS. The first, shown in Figure 3.1a, is a foam of hmC alone. Here, one barrel of the DBS contains a solution of hmC in 1.1 M $CH_3COOH$. The other barrel has a solution of 1.1 M $NaHCO_3$. The use of identical molarities for the acid and base ensures that the resulting foam will have a near-neutral pH, confirmed via a pH sensor. This hmC foam is similar to those created earlier, which were delivered through a canister. As mentioned in the Introduction, we explored a second foam formulation that combined hmC with hmA. Here, the DBS (Figure 3.1b) has one barrel that is the same as above, i.e., hmC in 1.1 M $CH_3COOH$. The second barrel has a solution of hmA in 1.1 M $NaHCO_3$. Our hypothesis was that the hmC-hmA foams would be more robust than the foams of hmC alone due to the electrostatic interactions between the two polymers.

Upon visual inspection, we found that the hmC-hmA foams indeed did have distinct mechanical properties compared to the hmC foams. To make a meaningful comparison, we fixed the total concentration of polymer at 4 wt% for the two sets of foams. That is, we compared a foam prepared with 4 wt% hmC in one barrel with a foam prepared using 2 wt% hmC and 2 wt% hmA in the two barrels. Visual comparisons of the two foams are shown in Figures 3.2 and 3.3. In Figure 3.2, the foams are placed on a flat surface. When a spatula is used to compress or tap the hmC foam, the bubbles in that area tend to dissipate and the foam collapses over the disturbed area. This shows the mechanical fragility of the hmC foam. In contrast, when the hmC-hmA foam is compressed with the spatula, that area deforms, but the foam does not dissipate or

collapse. Instead, this foam exhibits an elastic response and “pushes back” against the applied deformation. Thus, there are clear differences between the two foams.

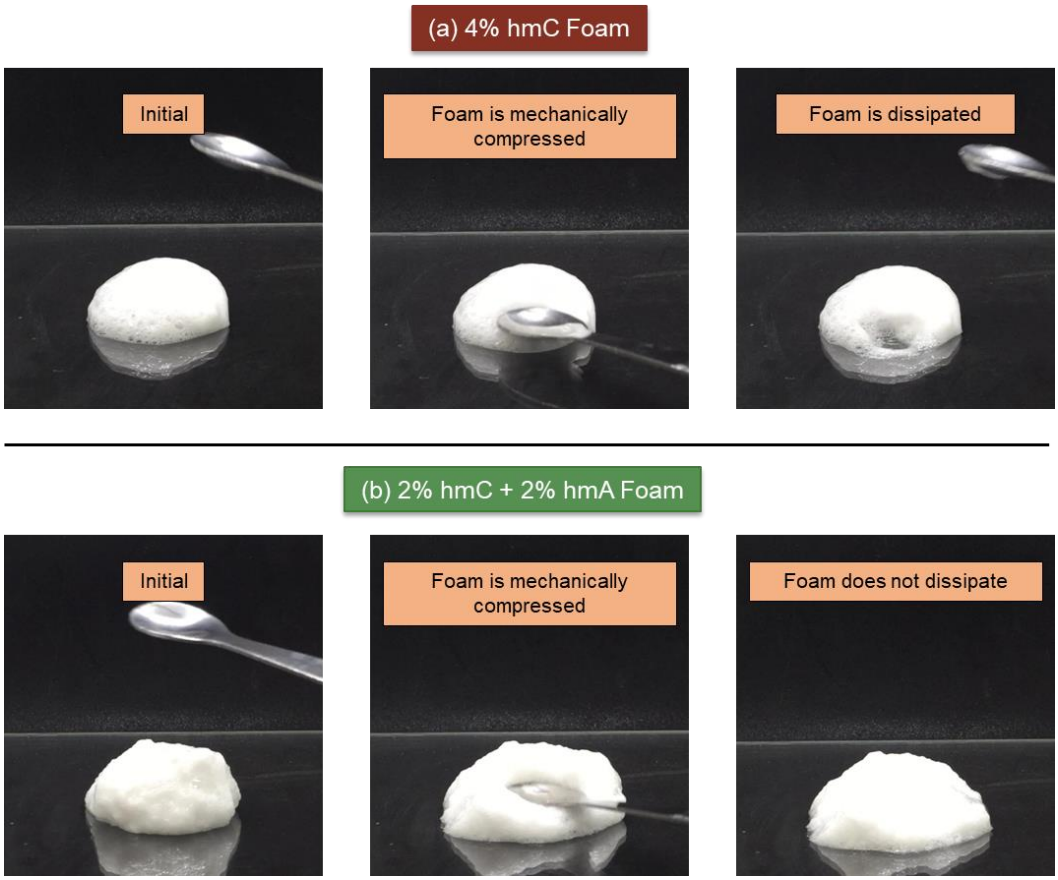


**Figure 3.2**: **Visual comparison of an hmC foam and an hmC-hmA foam.** Both have a total polymer concentration of 4 wt%. In each case, the sample is lightly tapped with a spatula. In (a), the bubbles dissipate in the tapped area and the foam collapses. In (b), the foam does not dissipate; rather it responds like an elastic object.

Figure 3.3 qualitatively shows the differences between the foams in a different way. Here, each foam is placed between parallel plates and the top plate is brought down to compress the foam. After compression to half its initial height for a minute, the top plate is retracted to its initial height. Figure 3.3a reveals that the compression causes a large fraction of the bubbles in the hmC foam to burst or dissipate. When the plate is raised back, the residue from the foam remains adhered to each plate, but most of the

bubbles have disappeared. This shows that the foam cannot withstand the compressive stress imposed on it. In contrast, when compression is applied on the hmC-hmA foam, the bubbles do not burst. When the plate is raised back, the foam sticks to the top plate as well, but the overall material retains its integrity despite the deformation.

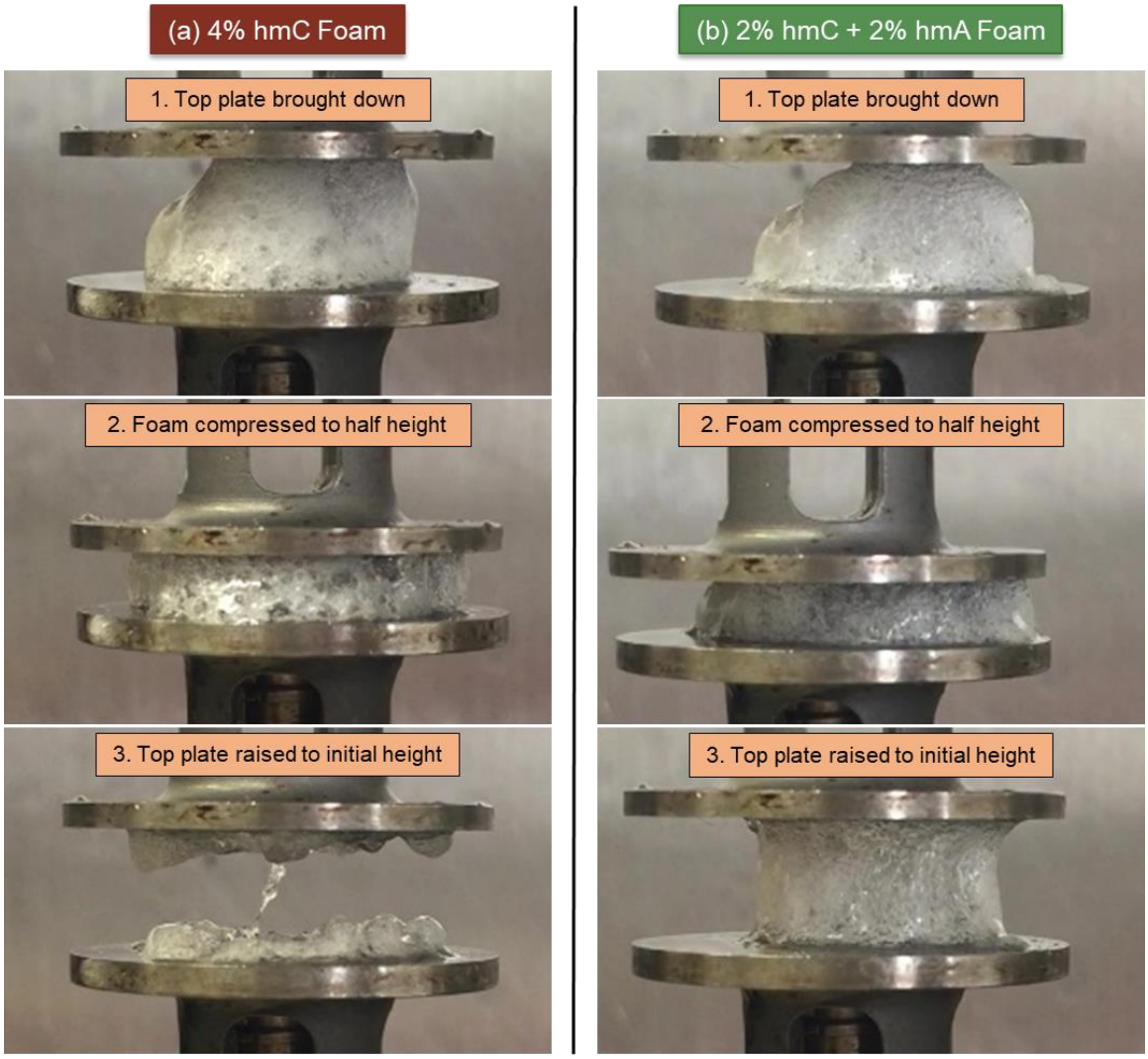


**Figure 3.3: Visual comparison of an hmC foam and an hmC-hmA foam subjected to compression between parallel plates.** Both have a total polymer concentration of 4 wt%. In each case, the sample is compressed to half its initial height for 1 min, then the top plate is raised back up. In (a), the compression causes bubbles to burst and the foam is dissipated by the end. In (b), the foam retains its integrity after the deformation.

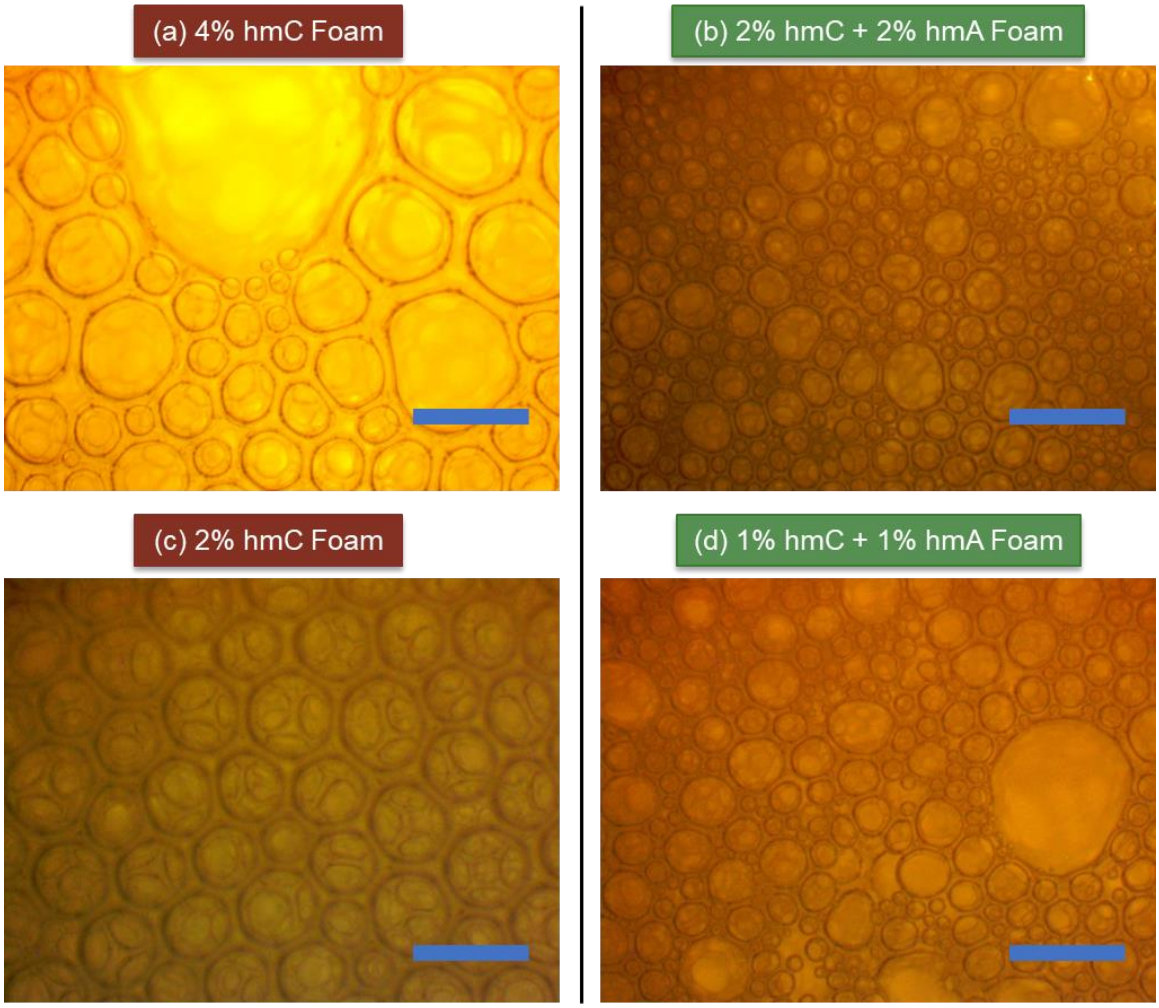


**Figure 3.4**: **Images from optical microscopy of foams with various polymer contents.** (a) 4% hmC; (b) 2% hmC + 2% hmA; (c) 2% hmC; and (d) 1% hmC + 1% hmA. All scale bars are 200 µm. Foams (a) and (b) have the same total polymer concentration, as do foams (c) and (d).

Next, we characterized the hmC and hmC-hmA foams by optical microscopy. Representative images are provided in Figure 3.4. Images of the hmC foams are shown at two hmC concentrations: 4% (Figure 3.4a) and 2% (Figure 3.4c). Bubble sizes from these images were analyzed using ImageJ and the distributions are shown in Figure 3.5a and 3.5c, respectively, for the above samples. The mean bubble diameter is ~ 100 µm for the hmC foams. For comparison, the images of hmC-hmA foams are shown for total polymer

concentrations of 4% (Figure 3.4b) and 2% (Figure 3.4d) and the corresponding bubble distributions are presented in Figure 3.5b and 3.5d. The hmC-hmA foams have numerous small bubbles and the mean bubble diameter is ~ 50 µm (i.e., approximately half that of the hmC foams). Also, there are very few bubbles larger than 150 µm in the hmC-hmA foams whereas there are many such bubbles in the hmC foams. Note also from the y-axes that there are far more bubbles in the hmC-hmA foams compared to the hmC ones.

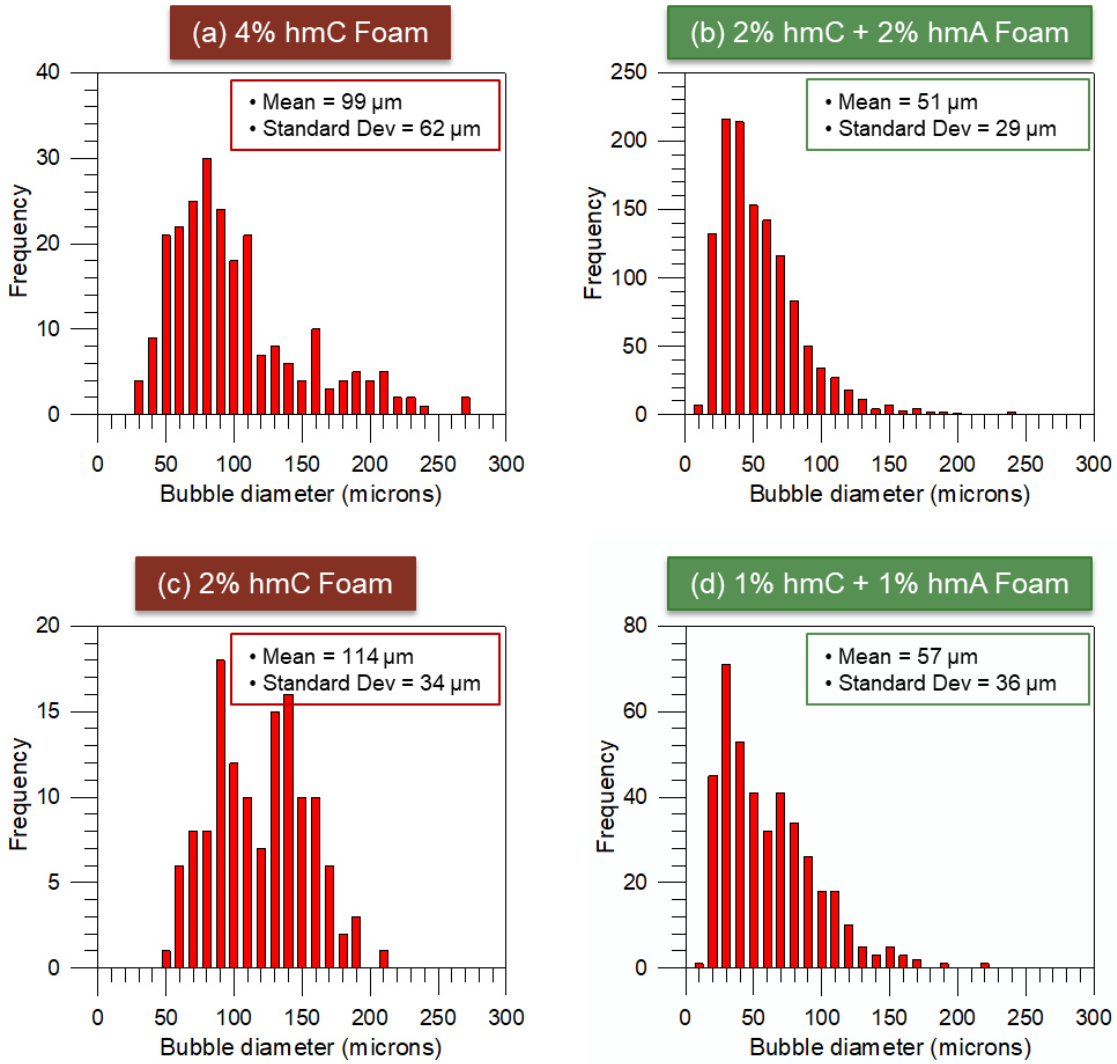


**Figure 3.5**: **Bubble size distributions for the various foams shown in Figure 3.4.** The plots are shown as histograms and were obtained by analyzing several microscope images of each foam.

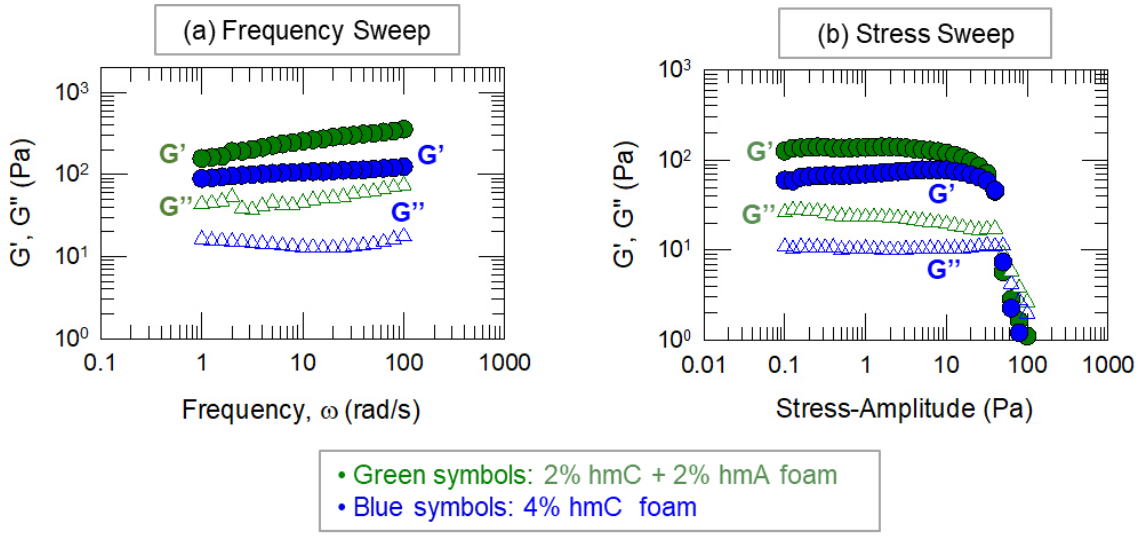


**Figure 3.6**: **Dynamic rheological comparison of an hmC and an hmC-hmA foam**. Both have the same total polymer content (4%). In the plots, the elastic modulus $G'$ (filled circles) and the viscous modulus $G''$ (unfilled triangles) are shown for the two samples. In (a), the moduli are plotted as functions of frequency. In (b), the moduli are plotted as functions of the stress-amplitude for a constant frequency of 10 rad/s.

We then proceeded to characterize the rheological properties of hmC and hmC-hmA foams. First, we compare foams with 4% hmC and 2% hmC + 2% hmA using dynamic rheology (oscillatory shear). Figure 3.6a plots the elastic modulus $G'$ and the viscous modulus $G''$ against frequency $\omega$. Both foams show $G' > G''$, with the moduli being nearly independent of frequency. This kind of response indicates the solid-like behavior of the foams at low deformations (within the linear viscoelastic regime of the samples). The key parameter for foams is the elastic modulus $G'$, which is ~ 250 Pa for the hmC+hmA foam and about 100 Pa for the hmC foam. Figure 3.6b shows $G'$ and $G''$ as functions of the stress-amplitude $\sigma$ for a constant frequency of 10 rad/s. The moduli are independent of $\sigma$ for low $\sigma$ (linear regime) and then beyond a critical $\sigma$ (i.e., the yield

stress), they rapidly decrease (non-linear regime). The yield stress is ~ 25 Pa for both foams, i.e., there are no significant differences in this parameter between the two.

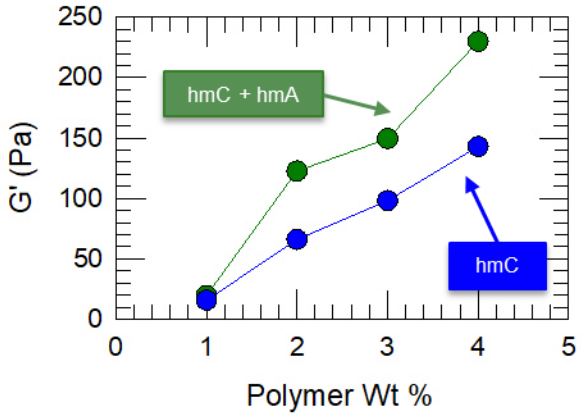


**Figure 3.7**: **Elastic moduli (*G′*) of hmC and hmC-hmA foams as a function of the total polymer concentration.** The hmC-hmA foams have equal concentrations of the two polymers that sum up to the concentration in the hmC foam. Each formulation was tested at least three times.

Next, we examine the relationship between the elastic modulus *G′* and the polymer concentration in the foam. We studied this for both the hmC and the hmC-hmA foams. The latter had equal concentrations of the two polymers – e.g., a 2% foam corresponded to 1% hmC + 1% hmA. Each sample was studied by dynamic rheology and the plotted values in Figure 3.7 correspond to a frequency of 10 rad/s. The results show that the hmC-hmA foams have higher *G′* values across the concentration range. Note that *G′* is a measure of the stiffness of the foam. Previous studies have correlated the foam modulus with the average bubble size and the number density of bubbles. Typically, the smaller the bubbles, and thereby the greater the number density of bubbles, the higher the foam modulus. In this regard, the data in Figures 3.4 and 3.5 do show that the hmC-hmA foams have smaller bubbles and also a higher number density of bubbles, which is

consistent with their higher $G'$ values (for a fixed total polymer concentration). If bubble size and density determine $G'$, what about the electrostatic interactions between hmC and hmA and their forming a PEC? We are not sure if the PEC contributes to the linear rheology of the foam. However, the PEC is expected to influence bubble coalescence, which could impact the non-linear rheology of the foam (see below).

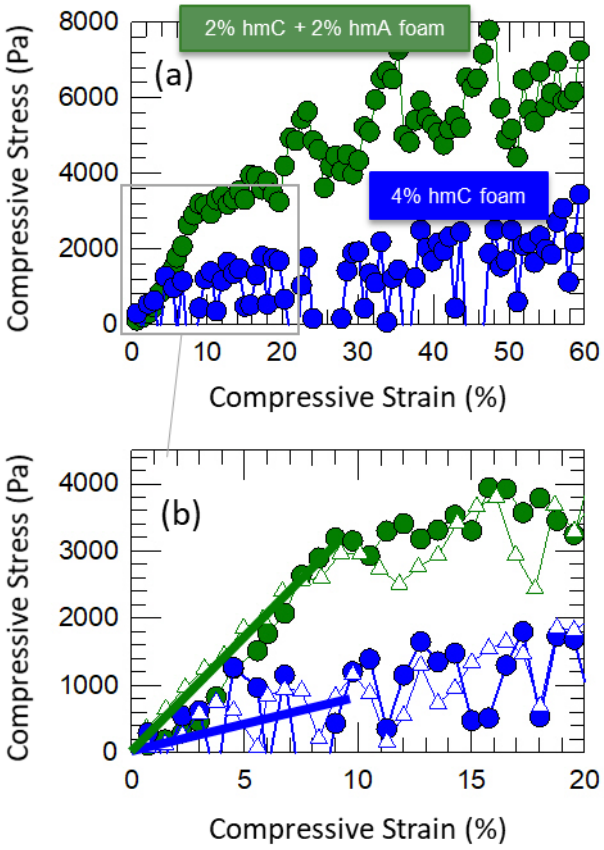


**Figure 3.8**: **Compression tests on an hmC and an hmC-hmA foam**. Both foams have the same total polymer content (4%). The data plotted are for the compressive stress vs. compressive strain. The data up to 60% strain are shown in (a). In (b), a close-up of the initial data is presented. Data from a second run on the same sample is additionally shown here. Also, a line is drawn through the data for each sample to roughly capture the slope of the initial linear region, which gives the compressive modulus.

In addition to shear, we also examined the foams under compression. In these tests, the foam is placed between parallel plates and compressed by a given amount,

which thereby yields the compressive strain. The force exerted by the sample on the top plate is recorded by a transducer and is converted into the compressive stress. Plots of compressive stress vs. compressive strain are shown in Figure 3.8 for the hmC and hmC-hmA foams. The data on both foams are irregular and exhibit abrupt peaks and valleys. We believe the irregularities are caused by bubble coalescence. Nevertheless, duplicate runs on the same sample show the same broad trends. The first key trend is that a much higher stress is required to compress the 2% hmC+ 2% hmA foam to a given extent compared to the 4% hmC foam. Also, over the initial strains (Figure 3.8b), the data for the hmC-hmA foam is relatively smooth and nearly linear, whereas a linear region is not so evident for the hmC foam. Still, we can infer from the slopes that the former has a higher compressive modulus (~ 35 kPa) compared to the latter (~ 10 kPa). Moreover, the linearity of the initial region for the hmC-hmA foam is consistent with the elastic response noted visually in Figure 3.2.

To gain further insight into foam properties, we went on to characterize two commercially available foams, and we will highlight the similarities between these materials and the foams made in the lab. The first is the Caress Botanicals Shower Foam (Figure 3.9a) and the second is the Gillette Foamy Shaving Foam (Figure 3.9b). Both are liquid foams that utilize propellants to generate gas bubbles and surfactants to stabilize them. In the case of the Caress foam, its visual appearance (Figure 3.9a, Panel 2) and its microstructure from optical microscopy (Panel 3) are both very similar to that of the 4% hmC foam (Figures 3.2a and 3.4a). Compression tests on this foam show a smooth overall response (Panel 4). From the initial slope, the compressive modulus is calculated

to be 2.5 kPa, which is lower than that of the 4% hmC foam. Correspondingly, a low stress of 300 Pa is sufficient to compress this foam to a 60% strain. This implies that the foam is mechanically fragile, much like the hmC foams.

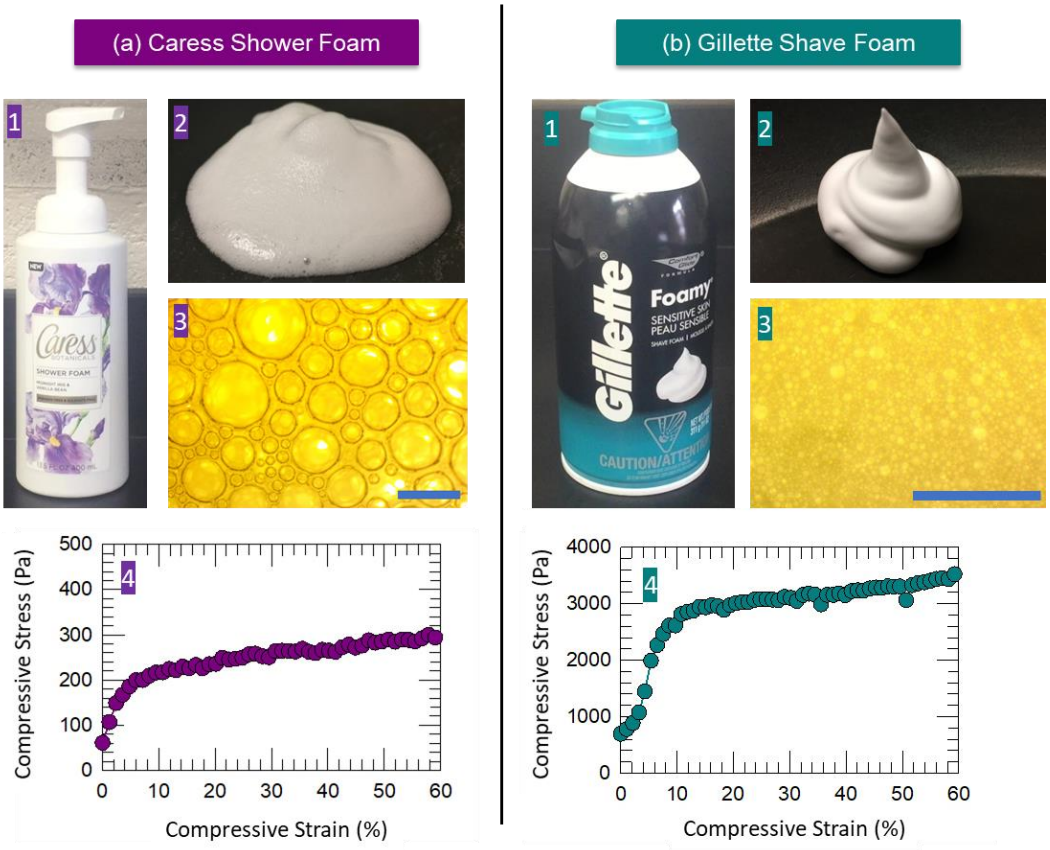


**Figure 3.9**: **Structure and properties of two commercial foams.** The foams are (a) Caress Botanicals Shower Foam and (b) Gillette Foamy Shave Foam. In both cases, a photo of the product is shown in Panel 1, a photo of the foam on the benchtop in Panel 2, an optical micrograph of the foam in Panel 3 (scale bars are 200 µm), and data from a compression test on the foam in Panel 4.

In the case of the Gillette foam, it has a mousse-like consistency (Figure 3.9b, Panel 2), and microscopy reveals that the bubbles in it are much smaller than all the other foam we studied (Panel 3). The small size also correlates with a very high bubble density, due to which the sample is nearly opaque, and this makes it difficult to identify the contours of the bubbles. As a result, the average bubble size cannot be easily determined.

Interestingly, the response of this foam to compression is quite similar to that of the 2% hmC + 2% hmA foam (Figure 3.8), albeit with much smoother data (Panel 4). The compressive modulus from the linear part of the curve is ~ 35 kPa, which is nearly identical to that of the hmC-hmA foam. Thus, much like the hmC-hmA foam, the Gillette foam is mechanically robust.

Our studies with the commercial foams give the following insights. Firstly, to obtain a high compressive stiffness and strength in the foam, it is usually required to reduce the bubble size to a small value, possibly less than 10 μm. This is exemplified by the Gillette foam, which thereby has the feel and consistency of a mousse. In the case of the hmC-hmA foams, we again observe a high compressive stiffness/strength even though the bubbles are relatively large. We believe this can be attributed to the electrostatic interactions between hmC and hmA. When the foam is compressed, the bubbles will be pushed together. However, for bubbles to coalesce, the liquid film between them must drain. Because of the hmC-hmA interactions, this liquid film is likely to be highly viscous or even gel-like. As a result, the film drainage will be suppressed, which could explain the resistance to compression, and thereby the mechanical integrity of hmC-hmA foams.

Our next step was to compare how the hmC and hmC-hmA foams interfaced with blood. A simple tube inversion test served as a preliminary indicator in this regard. For this, 10 mL of heparinized bovine blood was first added to a 50 mL centrifuge tube. The foam (volume of 2 mL in each barrel of the DBS = 4 mL total) was injected into the tube

from the nozzle of the DBS. The foam then expanded and filled the headspace in the tube. The tube was then inverted to see whether the foam could hold back the blood. The results are shown in Figure 3.10.

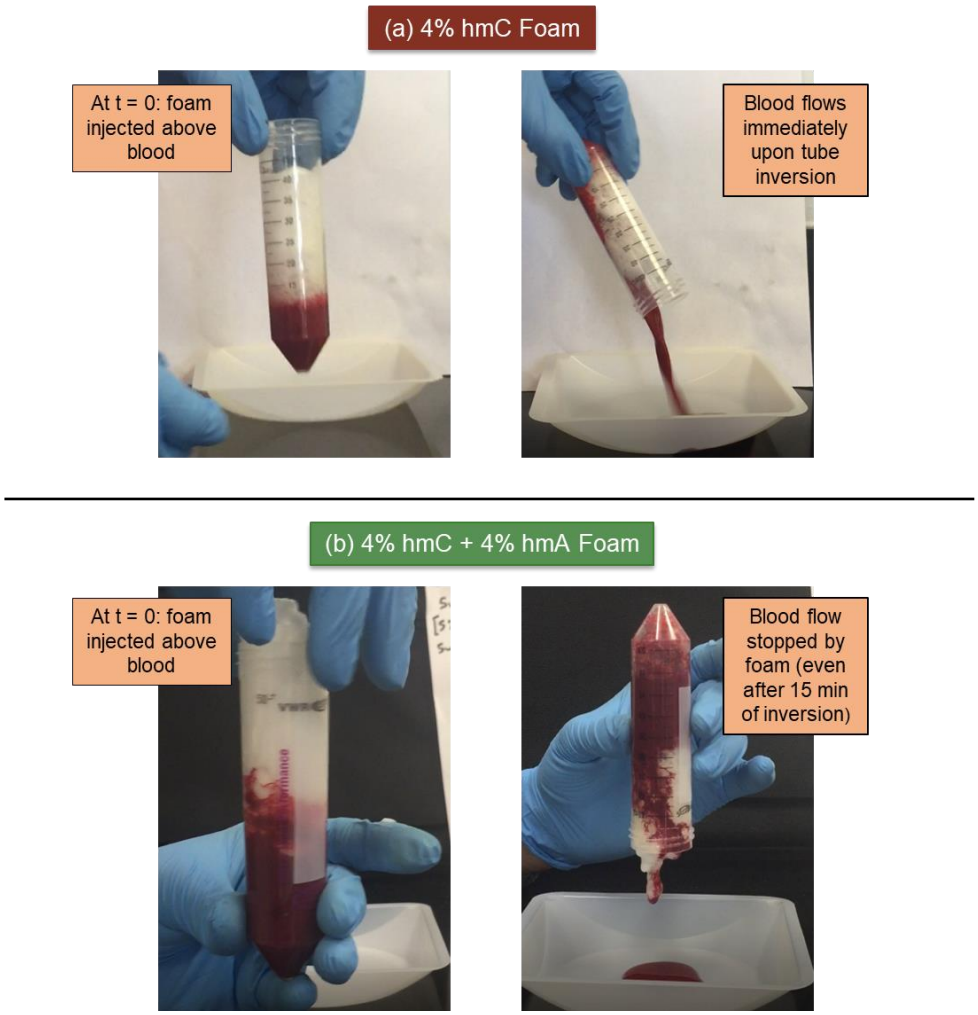


**Figure 3.10**: **Tube inversion test to examine foam-blood interactions.** Foams of (a) 4% hmC and (b) 2% hmC + 2% hmA are compared. In both cases, the foam is introduced over bovine blood in a tube at t = 0, and the tube is then immediately inverted to see if the foam can hold back the blood. The foam in (a) is unable to do so, whereas the foam in (b) holds back 20 mL of blood for over 15 min.

In the case of the 4% hmC foam, the blood immediately flowed through the foam upon tube inversion (Figure 3.10a). This indicates that the hmC foam does not constitute a sufficient mechanical barrier to blood flow. However, the foam of 2% hmC + 2% hmA

was able to hold back the blood in the inverted tube for several minutes, confirming its greater mechanical integrity. Increasing the polymer concentration to 4% hmC + 4% hmA was enough to hold back 10 mL of blood for over 20 min. We then doubled the amount of blood to 20 mL and repeated the test with this foam. The foam was able to hold back the blood flow for over 15 min (Figure 3.10b). The results support our original hypothesis that hmC-hmA foams could be advantageous for hemostatic purposes.

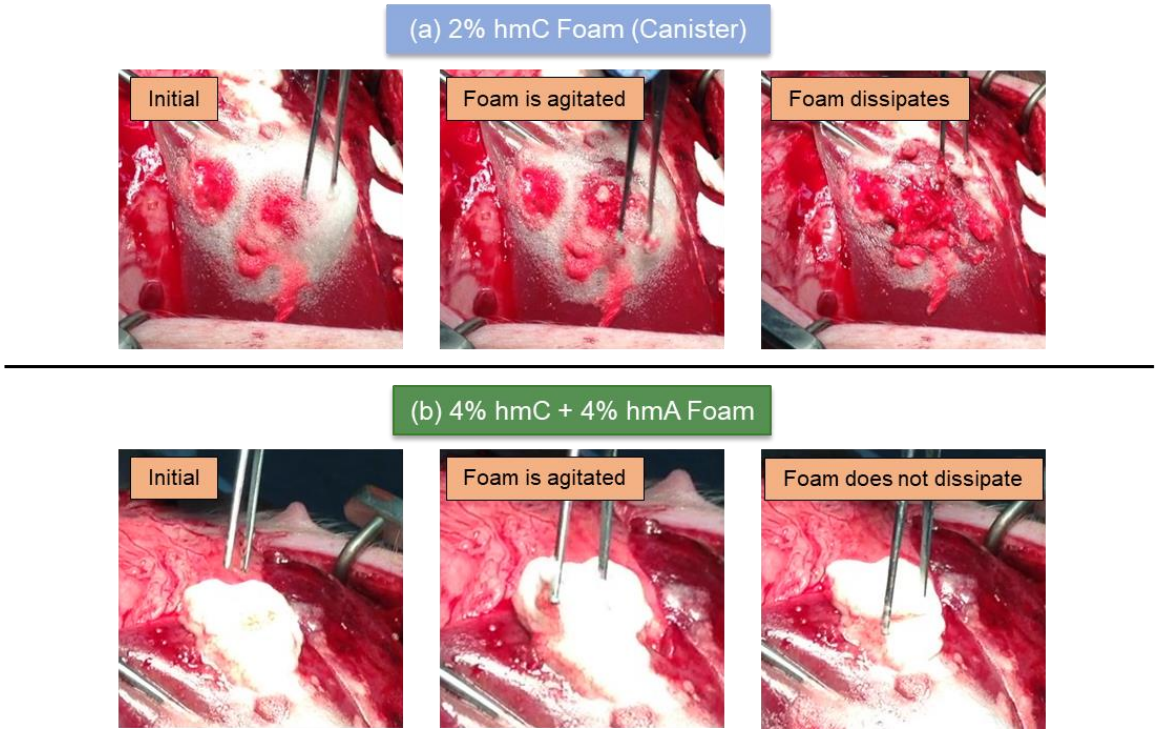


**Figure 3.11**: **Comparison of an hmC and an hmC-hmA foam as hemostatic agents over actively bleeding wounds in pigs**. (a) The hmC foam becomes saturated with blood and quickly dissipates when agitated with tweezers. (b) The hmC-hmA foam remains intact as a barrier to blood flow and does not dissipate when agitated.

Encouraged by these results, we proceeded to do some preliminary work to test the hemostatic efficacy of hmC-hmA foams in pig liver and spleen injury models. Initially we introduced a 2% hmC foam (out of a canister) and a 4% hmC+4% hmA foam (out of a DBS) over an actively bleeding pig injury (Figure 3.11). We then agitated both

foams using tweezers. Figure 3.11a shows that the canister foam becomes saturated with blood and dissipated upon agitation. In contrast, the hmC+hmA foam does not saturate with blood (i.e., it remains an intact barrier) and does not dissipate with agitation.

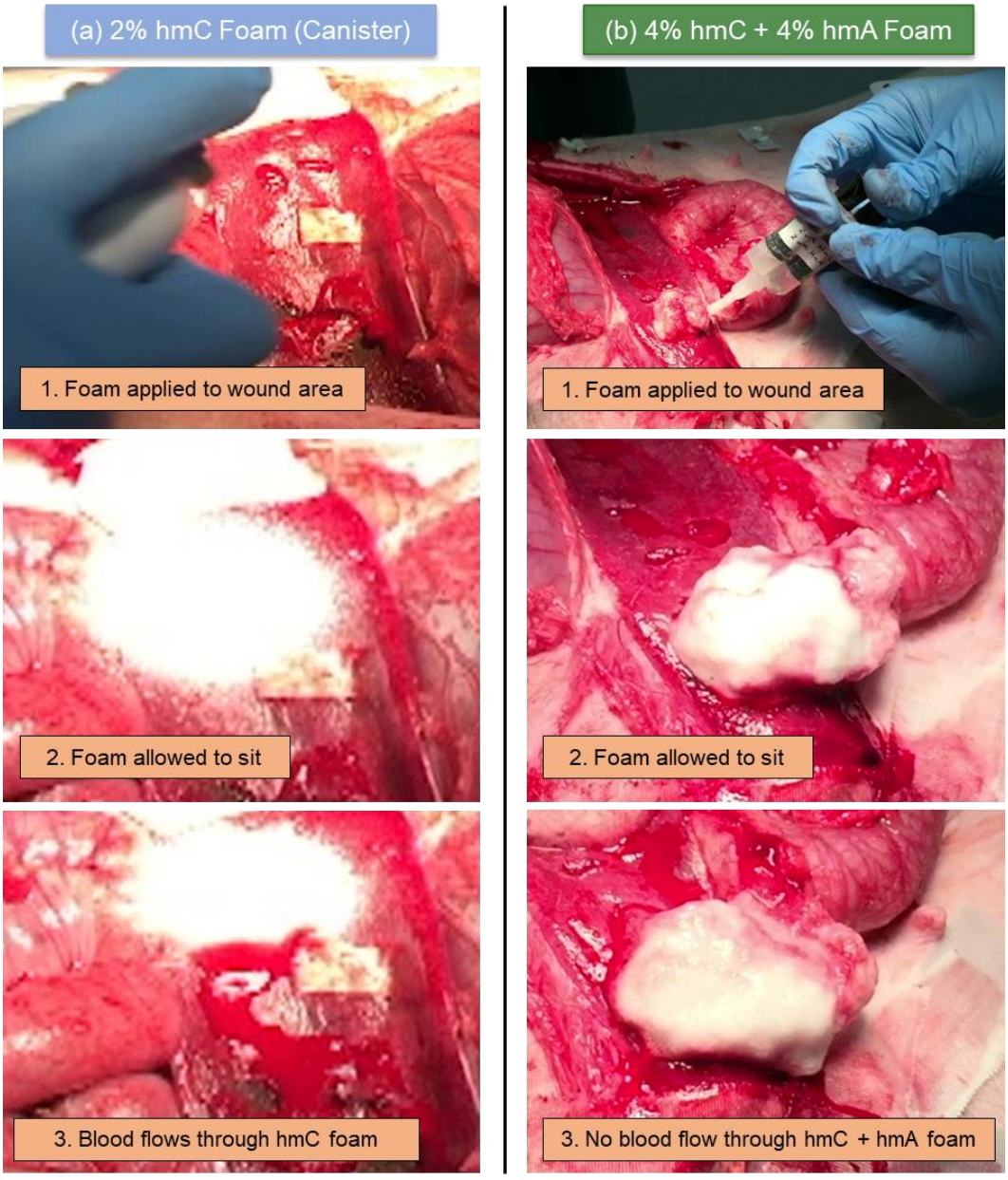


**Figure 3.12**: **Comparing the hemostatic properties of an hmC and an hmC-hmA foam against a pig liver injury**. The foams are applied to liver wounds made with dermal punches. (a) The hmC foam is unable to contain the bleeding, whereas the hmC-hmA foam remains as an intact barrier to blood flow over the same time frame.

Next, we applied both foams to a pig liver injury. Identical injuries were made using a 10 mm dermal punch and scissors, cutting a hole with a 10 mm diameter and a depth of several mm into the liver. Thereafter the foams were applied. We again found that the hmC foam held back the blood initially, but after a few minutes, the blood flowed through. In comparison, the hmC-hmA foam did not allow the blood to flow through over the same time frame. The results in Figures 3.11 and 3.12 show that the hmC+hmA foam has better barrier properties due to its greater mechanical integrity.

When testing both foams we observed that the hmC foam delivered out of the canister did have some attractive properties: it could quickly spread over a wide area and nicely wet the wound. This is a much desired feature in an ideal hemostat: it should quickly cover the wound but must not allow the blood to bleed through.[38] In comparison, it was difficult to get the hmC+hmA foam to fully cover and wet a large wound (this was partly because it was delivered out of a DBS than a canister, and partly due to its mechanical and wetting properties). These findings suggested that an optimal strategy could be to utilize both foams on the same injury to leverage both their strengths. A test with both foams was therefore conducted (see Figure 3.13). A liver injury was made as above with a 10 mm dermal punch. The hmC+hmA foam was first applied, quickly followed by the canister foam. This delivery allowed the hmC+hmA foam to serve as a robust barrier to the bulk of the blood flow while the canister foam completely covered the wound and surrounding area. The combination was allowed to sit for over 5 min, during which time no bleeding through the foams was observed. Then, the foams were removed, and even afterwards, no additional bleeding occurred, indicating that

hemostasis had been achieved. These results indicate that the combination of the two foams (hmC-hmA from the DBS and hmC alone from the canister) could be a viable strategy for the future to address large internal wounds. Further hemostatic tests will be needed to substantiate our preliminary results.

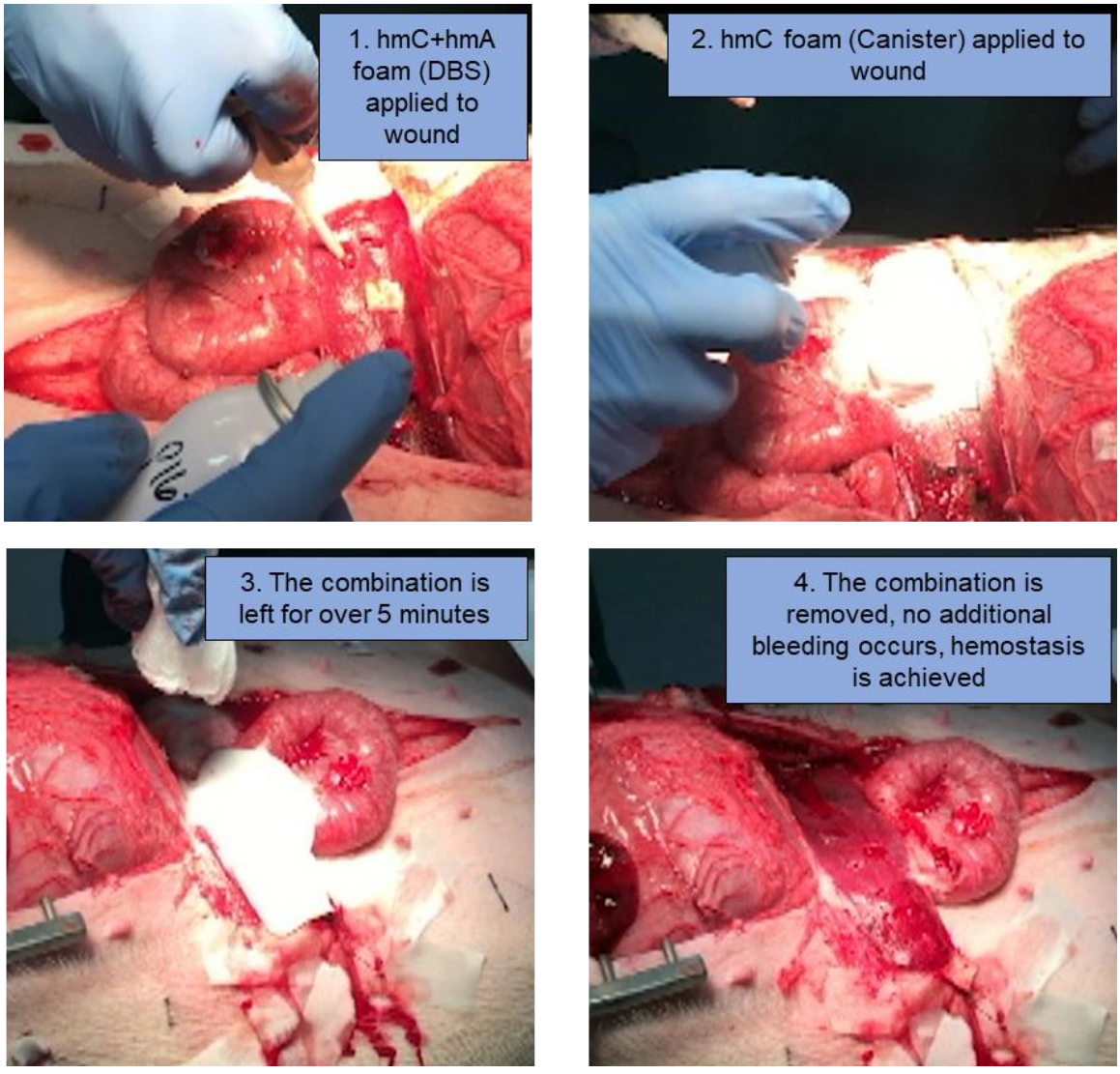


**Figure 3.13**: **Utilization of two foams concurrently on the same liver injury.** The hmC-hmA foam was first applied out of the DBS (1), then the hmC foam out of the canister (2). The combination proved successful in containing the bleeding (3), and hemostasis was achieved (4).

### 3.4 Conclusions

Our results show that foams based on mixtures of two hemostatic biopolymers, hmC (cationic) and hmA (anionic), are mechanically more robust than foams based on hmC alone. Both types of foams can be delivered through a double-barreled syringe (DBS), which produces a foam based on $CO_2$ at the mixing tip due to a reaction between acid and base. Compared to foams of hmC alone, the mixed hmC-hmA foams have smaller bubble sizes, greater bubble density, and in turn, higher elastic shear moduli. Compressive tests also reveal higher compressive moduli (stiffness) and strength; this also correlates with visual observations of the foams. Preliminary tests of the hmC+hmA foam in pig injury models again demonstrated clear advantages in its ability to form an intact barrier to blood leakage from the bleeding injuries. The barrier properties were related to the mechanical robustness of the foam. Overall, hmC-hmA foams are promising for future applications as hemostatic agents.

# Chapter 4: CONCLUSIONS & RECOMMENDATIONS

## 4.1 Conclusions

This research builds off of the discovery that hm-polymers can coagulate blood cells and stop bleeding from severe injuries. Our lab has shown that this technology can be utilized as a bandage to effectively combat compressible hemorrhaging. The next step in our work was to adapt this technology to treat non-compressible hemorrhaging, which despite being the minority of hemorrhaging cases accounts for the majority of hemorrhaging deaths. A foams ability to expand at a wound site and counteract hemorrhaging without compression makes it an attractive counter to non-compressible hemorrhaging. The amphiphilic nature of hm-polymers enables them to act as both a foam stabilizer and a hemostat. Our lab exploited this in our first attempt at hemostatic foams, which was centered around an hmC based foam delivered via a canister. By testing this foam we observed the need to develop foams that could be precisely placed and that had greater mechanical integrity.

The use of a DBS, which generates $CO_2$ gas via an *in situ* reaction between precursors in the respective barrels, allowed us to deliver foams precisely. We hypothesized that the combination of hmC and hmA would result in a more mechanically robust foam due to polymer-polymer interactions. The DBS allows us to exploit these interactions by mixing hmC in one barrel with hmA in a second. Through microscopy and rheology, we confirmed our hypothesis about the polymer-polymer interactions of hmC+hmA in foams. Foams with hmC+hmA have greater mechanical integrity than foams with only hmC. This was seen quantitively as foams with hmC+hmA had a higher

modulus than foams with only hmC. This rheological enhancement is due to electrostatic interactions between the cationic hmC and the anionic hmA chains. Preliminary studies on animal wound models also supports the qualitative and quantitative results obtained in the lab. This discovery lays the foundation for an exciting new direction for hemostatic foams. Given the promise of these foams, a number of additional experiments will be described that will help further this research.

### 4.2 Future Directions

**Systematic Animal Study.** Given the promise the hmC+hmA foams have shown a systematic animal study to evaluate the foams efficacy on non-compressible hemorrhages is warranted. Two pig wound models, a closed cavity femoral arterial puncture and a closed cavity liver excision, would provide valuable insight into the effectiveness of hmC+hmA foams and allow for a better understanding of the strengths and limitations of current formulations.

**Composition of Chitosan and Alginate.** Formulating the degree of association between ionic groups on chitosan and alginate has an impact on the PEC formed when the polymers interact.[24] It would be interesting to explore different alginate and chitosan compositions to see how PEC interactions affect the mechanical properties of the hmC+hmA foams. Additionally, using different length hydrophobic chains or different percent modifications may have an impact on the PEC's formed. This will affect the mechanical and hemostatic properties of the foam formed. Variations in hydrophobic chain length also likely have an impact on bubble size and distribution. We hypothesize that certain combinations of chain length will likely result in more dense, stable foams.

**Other Ionic Polymers.** A variety of polymers have ionic charges on their backbones and can be hydrophobically modified. These polymers could be paired with hmC or hmA in the context of the DBS and may result in foam with different mechanical properties than hmC+hmA foams. Characterizing these foams via rheological and qualitative tests could give insight into other potentially promising formulations of hemostatic foams.

**Volume Expansion and Stability.** It would be interesting to look at the volume expansion and stability hmC+hmA foams in comparison to hmC foams. Additionally, exploring how different chitosan and alginate formulations affect mechanical strength will also have impacts on foam stability. Having mechanically robust foams with long stability times is ideal when stabilizing a non-compressible hemorrhage as it may take a significant amount of time for the injured person to make it to a hospital.

[1] Martin, M.; Oh, J.; Currier, H.; Tai, N.; Beekley, A.; Eckert, M.; Holcomb, J. "An Analysis of In-Hospital Deaths at a Modern Combat Support Hospital." *The Journal of Trauma: Injury, Infection, and Critical Care* **2009**, *66*, S51-S61.

[2] Kauvar, D. S.; Lefering, R.; Wade, C. E. "Impact of Hemorrhage on Trauma Outcome: An Overview of Epidemiology, Clinical Presentations, and Therapeutic Considerations." *The Journal of Trauma: Injury, Infection, and Critical Care* **2006**, *60*, S3-S11.

[3] Kelly, J. F.; Ritenour, A. E.; McLaughlin, D. F.; Bagg, K. A.; Apodaca, A. N.; Mallak, C. T.; Pearse, L.; Lawnick, M. M.; Champion, H. R.; Wade, C. E.; Holcomb, J. B. "Injury Severity and Causes of Death From Operation Iraqi Freedom and Operation Enduring Freedom: 2003-2004 Versus 2006." *The Journal of Trauma: Injury, Infection, and Critical Care* **2008**, *64*, S21-S27.

[4] Stewart, R. M.; Myers, J. G.; Dent, D. L.; Ermis, P.; Gray, G. A.; Villarreal, R.; Blow, O.; Woods, B.; McFarland, M.; Garavaglia, J.; Root, H. D.; Pruitt, B. A. "Seven Hundred Fifty-Three Consecutive Deaths in a Level I Trauma Center: The Argument for Injury Prevention." *The Journal of Trauma: Injury, Infection, and Critical Care* **2003**, *54*, 66-71.

[5] Dowling, M. B.; MacIntire, I. C.; White, J. C.; Narayan, M.; Duggan, M. J.; King, D. R.; Raghavan, S. R. "Sprayable Foams Based on an Amphiphilic Biopolymer for Control of Hemorrhage Without Compression." *ACS Biomaterials Science & Engineering* **2015**, *1*, 440-447.

[6] Dowling, M. B.; Smith, W.; Balogh, P.; Duggan, M. J.; MacIntire, I. C.; Harris, E.; Mesar, T.; Raghavan, S. R.; King, D. R. "Hydrophobically-modified chitosan foam: description and hemostatic efficacy." *Journal of Surgical Research* **2015**, *193*, 316-323.

[7] Simmons, J. W.; White, C. E.; Eastridge, B. J.; Holcomb, J. B.; Perkins, J. G.; Mace, J. E.; Blackbourne, L. H. "Impact of Improved Combat Casualty Care on Combat Wounded Undergoing Exploratory Laparotomy and Massive Transfusion." *The Journal of Trauma: Injury, Infection, and Critical Care* **2011**, *71*, S82-S86.

[8] Holcomb, J. B.; McClain, J. M.; Pusateri, A. E.; Beall, D.; Macaitis, J. M.; Harris, R. A.; MacPhee, M. J.; Hess, J. R. "Fibrin Sealant Foam Sprayed Directly on Liver Injuries Decreases Blood Loss in Resuscitated Rats." *The Journal of Trauma: Injury, Infection, and Critical Care* **2000**, *49*, 246-250.

[9] Hawksworth, J. S.; Elster, E. A.; Fryer, D.; Sheppard, F.; Morthole, V.; Krishnamurthy, G.; Tomori, T.; Brown, T. S.; Tadaki, D. K. "Evaluation of lyophilized platelets as an infusible hemostatic agent in experimental non-compressible hemorrhage in swine." *Journal of Thrombosis and Haemostasis* **2009**, *7*, 1663-1671.

[10] Beekley, A. C.; Sebesta, J. A.; Blackbourne, L. H.; Herbert, G. S.; Kauvar, D. S.; Baer, D. G.; Walters, T. J.; Mullenix, P. S.; Holcomb, J. B. "Prehospital Tourniquet Use in Operation Iraqi Freedom: Effect on Hemorrhage Control and Outcomes." *The Journal of Trauma: Injury, Infection, and Critical Care* **2008**, *64*, S28-S37.

[11] English, R. J.; Raghavan, S. R.; Jenkins, R. D.; Khan, S. A. "Associative polymers bearing n-alkyl hydrophobes: Rheological evidence for microgel-like behavior." *Journal of Rheology* **1999**, *43*, 1175-1194.

[12] Panmai, S.; Prud'homme, R. K.; Peiffer, D. G. "Rheology of hydrophobically modified polymers with spherical and rod-like surfactant micelles." *Colloids and Surfaces A: Physicochemical and Engineering Aspects* **1999**, *147*, 3-15.

[13] Ashbaugh, H.; Boon, K.; Prud'homme, R. "Gelation of "catanionic" vesicles by hydrophobically modified polyelectrolytes." *Colloid & Polymer Science* **2002**, *280*, 783-788.

[14] Chen, Y.; Javvaji, V.; MacIntire, I. C.; Raghavan, S. R. "Gelation of Vesicles and Nanoparticles Using Water-Soluble Hydrophobically Modified Chitosan." *Langmuir* **2013**, *29*, 15302-15308.

[15] Bratskaya, S.; Avramenko, V.; Schwarz, S.; Philippova, I. "Enhanced flocculation of oil-in-water emulsions by hydrophobically modified chitosan derivatives." *Colloids and Surfaces A: Physicochemical and Engineering Aspects* **2006**, *275*, 168-176.

[16] Chiu, Y.-L.; Chen, M.-C.; Chen, C.-Y.; Lee, P.-W.; Mi, F.-L.; Jeng, U. S.; Chen, H.-L.; Sung, H.-W. "Rapidly in situ forming hydrophobically-modified chitosan hydrogels via pH-responsive nanostructure transformation." *Soft Matter* **2009**, *5*, 962.

[17] Cooney, M. J.; Petermann, J.; Lau, C.; Minteer, S. D. "Characterization and evaluation of hydrophobically modified chitosan scaffolds: Towards design of enzyme immobilized flow-through electrodes." *Carbohydrate Polymers* **2009**, *75*, 428-435.

[18] Dowling, M. B.; Javvaji, V.; Payne, G. F.; Raghavan, S. R. "Vesicle capture on patterned surfaces coated with amphiphilic biopolymers." *Soft Matter* **2011**, *7*, 1219-1226.

[19] Dowling, M. B.; Kumar, R.; Keibler, M. A.; Hess, J. R.; Bochicchio, G. V.; Raghavan, S. R. "A self-assembling hydrophobically modified chitosan capable of reversible hemostatic action." *Biomaterials* **2011**, *32*, 3351-3357.

[20] Iversen, C.; Kjøniksen, A.-L.; Nyström, B.; Nakken, T.; Palmgren, O.; Tande, T. "Linear and nonlinear rheological responses in aqueous systems of hydrophobically modified chitosan and its unmodified analogue." *Polymer Bulletin* **1997**, *39*, 747-754.

[21] Lee, J. H.; Gustin, J. P.; Chen, T. H.; Payne, G. F.; Raghavan, S. R. "Vesicle-biopolymer gels: Networks of surfactant vesicles connected by associating biopolymers." *Langmuir* **2005**, *21*, 26-33.

[22] De Castro, G. P.; Dowling, M. B.; Kilbourne, M.; Keledjian, K.; Driscoll, I. R.; Raghavan, S. R.; Hess, J. R.; Scalea, T. M.; Bochicchio, G. V. "Determination of efficacy of novel modified chitosan sponge dressing in a lethal arterial injury model in swine." *The Journal of Trauma Injury Infection and Critical Care* **2012**, *72*, 899-907.

[23] Dowling, M. B.; Chaturvedi, A.; MacIntire, I. C.; Javvaji, V.; Gustin, J.; Raghavan, S. R.; Scalea, T. M.; Narayan, M. "Determination of efficacy of a novel alginate dressing in a lethal arterial injury model in swine." *Injury* **2016**, *47*, 2105-2109.

[24] Lawrie, G.; Keen, I.; Drew, B.; Chandler-Temple, A.; Rintoul, L.; Fredericks, P.; Grøndahl, L. "Interactions between Alginate and Chitosan Biopolymers Characterized Using FTIR and XPS." *Biomacromolecules* **2007**, *8*, 2533-2541.

[25] Raafat, D.; von Bargen, K.; Haas, A.; Sahl, H. G. "Insights into the Mode of Action of Chitosan as an Antibacterial Compound." *Applied and Environmental Microbiology* **2008**, *74*, 3764-3773.

[26] Rabea, E. I.; Badawy, M. E. T.; Stevens, C. V.; Smagghe, G.; Steurbaut, W. "Chitosan as Antimicrobial Agent: Applications and Mode of Action." *Biomacromolecules* **2003**, *4*, 1457-1465.

[27] Elsabee, M. Z.; Abdou, E. S. "Chitosan based edible films and coatings: A review." *Materials Science and Engineering: C* **2013**, *33*, 1819-1841.

[28] Goy, R. C.; Britto, D. d.; Assis, O. B. G. "A review of the antimicrobial activity of chitosan." *Polímeros* **2009**, *19*, 241-247.

[29] Javvaji, V.; Dowling, M. B.; Oh, H.; White, I. M.; Raghavan, S. R. "Reversible gelation of cells using self-assembling hydrophobically-modified biopolymers: towards self-assembly of tissue." *Biomaterials Science* **2014**, *2*, 1016.

[30] Martin, A.; Grolle, K.; Bos, M.; Stuart, M.; Vanvliet, T. "Network Forming Properties of Various Proteins Adsorbed at the Air/Water Interface in Relation to Foam Stability." *Journal of Colloid and Interface Science* **2002**, *254*, 175-183.

[31] Marze, S. P. L.; Saint-Jalmes, A.; Langevin, D. "Protein and surfactant foams: linear rheology and dilatancy effect." *Colloids and Surfaces A: Physicochemical and Engineering Aspects* **2005**, *263*, 121-128.

[32] Marze, S.; Guillermic, R. M.; Saint-Jalmes, A. "Oscillatory rheology of aqueous foams: surfactant, liquid fraction, experimental protocol and aging effects." *Soft Matter* **2009**, *5*, 1937.

[33] Weaire, D. "The rheology of foam." *Current Opinion in Colloid & Interface Science* **2008**, *13*, 171-176.

[34] Marinova, K. G.; Basheva, E. S.; Nenova, B.; Temelska, M.; Mirarefi, A. Y.; Campbell, B.; Ivanov, I. B. "Physico-chemical factors controlling the foamability and foam stability of milk proteins: Sodium caseinate and whey protein concentrates." *Food Hydrocolloids* **2009**, *23*, 1864-1876.

[35] Salonen, A.; In, M.; Emile, J.; Saint-Jalmes, A. "Solutions of surfactant oligomers: a model system for tuning foam stability by the surfactant structure." *Soft Matter* **2010**, *6*, 2271.

[36] Asari, M.; Hormozi, F. "Experimental Determination of Bubble Size in Solution of Surfactants of the Bubble Column." *Journal of Advanced Chemical Engineering* **2014**, *04*.

[37] K. Prud'homme, R., A.Khan, S *Foams: Theory, Measurement and Application*; CRC Press 1995; Vol. 57.

[38] Greff, R. J.Cross-linked gelatin composition comprising a wetting agent. US8821918B2, March 12, **2001**. (US Patent)